

AN ABSTRACT OF THE THESIS OF

DWIGHT POCOCK CLARK for the Ph. D. in Chemical Engineering
(Name) (Degree) (Major)

Date thesis is presented August 27, 1964

Title THERMALLY ACTIVATED ELECTROCHEMICAL CELLS
USING A STABILIZED ZIRCONIA ELECTROLYTE

Abstract approved Redacted for Privacy
(Major professor)

The performance of solid metallic anodes on a solid electrolyte was determined experimentally and data on cell current, cell voltage, open-circuit cell potential, and cell energy are presented. Fifteen-mole percent calcia-stabilized zirconia was used as the electrolyte, a platinum-oxygen electrode was used as the cathode, and 1000° C was the operating temperature for all cells tested.

The cells were built around a zirconia crucible, one-inch diameter and approximately 1/16 inch thick. The cathode was applied to the inside base of the crucible and the anode to the outside base. The anode was applied by a two-step process. First, a thin layer of the metal being studied was deposited by vacuum evaporation techniques, and second, the film was thickened using published electroplating procedures.

Attempts to fabricate cells using iron, nickel, cobalt, manganese, chromium, molybdenum, zirconium, yttrium, and a zirconium-

yttrium mixture were successful only in the case of the first four elements. The cells were tested in a tube furnace with controlled cathodic and anodic atmospheres. The measured open-circuit voltages were in satisfactory agreement with the theoretical values determined from standard free energy data at 1000° C.

All the cells behaved as secondary batteries, in that they could be recharged a number of times following the initial discharge. Data obtained for the iron and nickel cells established the reproducibility of the experimental procedures used in this work.

THERMALLY ACTIVATED ELECTROCHEMICAL CELLS
USING A STABILIZED ZIRCONIA ELECTROLYTE

by

DWIGHT POCOCK CLARK

A THESIS

submitted to

OREGON STATE UNIVERSITY

in partial fulfillment of
the requirements for the
degree of

DOCTOR OF PHILOSOPHY

August 1964

APPROVED:

Redacted for Privacy

Associate Professor of Chemical Engineering

In Charge of Major

Redacted for Privacy

Head of Department of Chemical Engineering

Redacted for Privacy

Dean of Graduate School

Date thesis is presented August 27, 1964

Typed by Lucinda Nyberg

ACKNOWLEDGMENTS

If I were to mention by name all those who helped to bring this work to completion, the list would be seemingly endless. However, I especially wish to express my gratitude to Professor R. E. Meredith for his valued council and encouragement, and for the freedom he gave me during the course of this work: to Professor R. V. Mrazek for his valued assistance in writing this thesis, and to Professors W. M. Stone and A. B. Scott for their review of this thesis.

I am indebted to my friends at the U. S. Bureau of Mines, Albany, Oregon, especially Raymond L. Carpenter, Henry M. Harris, John Kelley, and Gabriel Robidart for their technical assistance in solving many of the problems associated with high temperatures and vacuum equipment, and for their generosity in contributing some of the crucibles and anodic metals used in this work.

Grateful acknowledgments are also given to the Naval Ordnance Laboratory, Corona, California, for funding this project, and to the American people for my three-year NDEA fellowship.

I am grateful to John Darrah for his help in the final testing of my vacuum system, and to the OSU Department of Physics for the use of their helium leak detector.

Finally, I wish to thank my wife, Bertha, for her love, patience, understanding, and encouragement during the course of this work, and for her many hours at the typewriter at the conclusion of this work.

TABLE OF CONTENTS

	Page
INTRODUCTION	1
Statement of the Problem	3
Scope of this Work	8
LITERATURE REVIEW	10
FABRICATION OF CELLS	19
Cell Design	19
Cell Construction	20
EXPERIMENTAL PROCEDURE FOR CELL TESTING	26
EXPERIMENTAL RESULTS	39
DISCUSSION OF RESULTS	51
The Flat Section of the Discharge Curves	51
The Initial Prominence of the Discharge Curve	53
CONCLUSIONS	61
RECOMMENDATIONS FOR FUTURE STUDY	62
BIBLIOGRAPHY	63
APPENDIX	
I. Selection of Anodes	65
II. Anode Film Construction	73
Iron Anode	73
Nickel Anode	74
Molybdenum Anode	74
Zirconium and Yttrium Anodes	75
Manganese Anode	76
Cobalt Anode	76
Chromium Anode	77

LIST OF FIGURES

Figure		Page
1	A reproduction of Figure 5 in the paper by Tien (17), which is a presentation of isothermal conductivity - composition data for the system $\text{ZrO}_2 - \text{CaZrO}_3$	12
2	A reproduction of Figure 19 in a paper by Archer et al (2), which is a presentation of the conductivity at 1000°C vs. composition for $(\text{ZrO}_2)_{1-x}(\text{CaO})_x$, where $0.1 < x < 0.25$ and $(\text{ZrO}_2)_{1-x}(\text{Y}_2\text{O}_3)_x$, where $0.05 < x < 0.25$	13
3	Photograph of the assembled vacuum equipment. .	22
4	Photograph of crucible cell ready for testing. Pictured also is the end of the stabilized zirconia work tube. One of the monitoring electrodes can be seen on the right side of the crucible.	30
5	Sectional close-up sketch showing cell assembly inside the furnace	31
6	Sectional sketch showing cell assembly inside of the furnace	32
7	Photographs showing the arrangement of the refractory tube seal and Swagelok fittings on one end of the system. Visible also are the Mullite and stabilized zirconia work tubes, and the spring-loaded clamp on the small alumina tube	33
8	Photograph of the equipment used for cell testing. Visible are the tube furnace with tube assembly, two-channel recorder, terminal board, and oscilloscope with camera attachment	36
9	Circuit diagram for cell testing	37
10	Discharge curves for the cell $\text{Fe}/\text{Stab. Zirc.}/\text{Pt}, \text{O}_2$	41
11	Discharge curves for the cell $\text{Fe}/\text{Stab. Zirc.}/\text{Pt}, \text{O}_2$	42

Figure		Page
12	Discharge curves for the cell Ni/Stab. Zirc. /Pt, O ₂	43
13	Discharge curves for the cell Ni/Stab. Zirc. /Pt, O ₂	44
14	Discharge curves for the cell Mn/Stab. Zirc. /Pt, O ₂	45
15	Discharge curves for the cell Mn/Stab. Zirc. /Pt, O ₂	46
16	Discharge curves for the cell Co/Stab. Zirc. /Pt, O ₂	47
17	Discharge curves for the cell Co/Stab. Zirc. /Pt, O ₂	48
18	Reproducibility of data for iron and nickel anodes discharged through a fixed resistance.	49
19	Photograph of an oscilloscope trace obtained while forcing a current pulse through the cell O ₂ , Pt/Stab. Zirc. /Pt, O ₂ . The vertical scale is 0.05 volts/cm. The horizontal scale is 0.1 milli- second/cm. The small squares are one centimeter square	54

LIST OF TABLES

Table		Page
I	ENERGY OUTPUT AND OPEN CIRCUIT POTENTIAL OF EACH CELL TESTED	50
II	SOME THERMODYNAMIC PROPERTIES OF THE METALS AND THEIR OXIDES AT 1273°K	68

THERMALLY ACTIVATED ELECTROCHEMICAL CELLS USING A STABILIZED ZIRCONIA ELECTROLYTE

INTRODUCTION

In recent years a considerable amount of research has been conducted to find better methods and devices for producing energy in a useable form from naturally occurring or commercially synthesized materials (10). Since the efficiency of any device utilizing the thermal energy of a fuel has the Carnot efficiency as its upper limit, special emphasis has been placed on developing electrochemical devices (1, 10), that is, fuel cells and batteries,¹ which would convert the chemical energy of various substances directly into electrical energy and which are not limited by the Carnot efficiency. Other things being equal, this increase in efficiency brings about an increase in the overall efficiency of the energy producing device, hence, a decrease in the system's weight per unit of energy produced. This last factor is of paramount importance in the equipment used for space exploration, and establishes one of the reasons for conducting research in this general area. The problem of containing the

¹Throughout this dissertation the term fuel cell will signify a type of battery in which the electrochemical reactants are continuously fed to the separate electrodes during operation of the cell; the term battery will have its usual meaning, as for example the lead-acid storage battery.

electrolyte in a weightless environment establishes the need for a solid electrolyte, and the problem of transporting the fuel and oxidizer to their respective reaction sites in a weightless environment establishes the need for solid electrodes which are also the reactants. Undoubtedly, other reasons could be given but these were sufficient to establish the need for conducting the research as described in this dissertation.

Since the operating temperature affects the conductivity of the electrolyte and also dictates the ultimate design of the working cell, fuel cells and batteries are roughly grouped according to this parameter. Hence, there are low temperature cells, medium temperature cells, and high temperature cells. The three temperature ranges are quite arbitrarily assigned. One could consider certain ammonia batteries as examples of low temperature cells, the common dry cell and lead-acid storage battery as examples of medium temperature cells, and fused salt cells as examples of high temperature cells. The high temperature group also includes many cells which employ solid electrolytes, as for example, the Austin cell (3).

More than sixty years ago, Nernst (14) discovered that the solid solution known as the Nernst - Mass, which is composed of 85 weight percent zirconia and 15 weight percent yttria, possessed a relatively high ionic conductivity at high temperatures. Nernst observed the electrolytic evolution of oxygen from a rod of this material and thus

demonstrated that its ionic conductivity was due largely to migrating oxide ions. This solution is possibly the best known oxygen-ion-conducting solid electrolyte and undoubtedly the earliest one discovered. The Nernst - Mass and similar solids employing calcia or magnesia in place of yttria, have received considerable attention recently as possible solid electrolytes in fuel cells having gaseous reactants. (For example, Archer and co-workers (2) of Westinghouse Electric Company are carrying out an investigation of solid-electrolyte fuel cells using stabilized zirconia as the electrolyte and hydrogen as the fuel.) The properties of these electrolytes have therefore been studied quite extensively.

Statement of the Problem

Presintered, calcia-stabilized, zirconia has been and is being used as a solid electrolyte in a number of high temperature fuel cells (1, 2, 3, 21). No one, to the author's knowledge, has attempted to use this material as an electrolyte in a solid state battery. However, the concept of using a solid electrolyte in an air-depolarized solid-state battery is actually not a new one. For example, the Austin cell (3) has this same general configuration. However, it is built around a lithium borosilicate glass electrolyte rather than the stabilized zirconia electrolyte, and its operating temperature is much lower (less than 500° C). The Austin type cells in general are beset

with problems peculiar to a solid state battery, for example, anodic polarization during discharge, anode-electrolyte and cathode-electrolyte separation during cell operation, and initial bonding of the electrodes to the electrolyte.

Anodic polarization is probably the chief problem in this application. To illustrate this, one might consider the oxidation of aluminum. In the oxidation of aluminum it is well known that only a very thin film of alumina will form at ordinary temperatures because of the high field required for any significant ionic transport through the film. If this film were to be removed as soon as it formed, the oxidation of the aluminum would proceed until no more aluminum metal was available for oxidation. If aluminum were used as an anode in an electrochemical device, the amount of current which could be drawn from this cell would therefore depend on the amount of aluminum available for the electrochemical oxidation, because the entire aluminum anode could be consumed during the cell discharge if the electrolyte were capable of dissolving the alumina formed. If, however, the electrolyte were incapable of dissolving any of the alumina, the alumina film formed would quickly polarize the cell, and only a small amount of current could be drawn from the cell. This same discussion could be applied to any metal used as the anode in an electrochemical cell. (Of course, with a liquid electrolyte, the anodic reaction product would not need to be dissolved but would merely have to be sufficiently

porous to maintain the electrode-electrolyte contact. An example of this type of mechanism would be found in the lead-acid storage battery.)

With the Austin cell, the electrolyte is somewhat fluid at the operating temperature of the cell and is capable of dissolving some of the anodic reaction products. However, calcia-stabilized zirconia at 1000°C is still a solid and only a very insignificant amount of the metal oxide will dissolve (or diffuse) at the anode during the discharge of the cell.

The thickness of the oxide film on a metal surface exposed to oxygen increases with increasing temperature. In addition to this, there are metals which continue to oxidize even after the film has an appreciable thickness. For example, silver forms silver chloride in chlorine. This is due to the mobility of one of the ions through the lattice of the reaction product.

It was with these thoughts in mind that this study was initiated. The investigations thus consisted of testing various metallic anodes to determine the amount of power one could get from a cell during the build-up of the oxide film on the anode at elevated temperatures. In order to carry out such a study, a method had to be devised for constructing the cell. The problem of attaining intimate contact between the electrodes and the electrolyte and maintaining that contact during cell operation had to be solved since any separation would prevent an electrochemical reaction from occurring. If the electrodes were

joined to the electrolyte at ordinary temperatures, they would either try to assume the basic crystal structure of the electrolyte or some other structure natural to the substance in question. In either case, because of the differences in thermal expansion properties existing between the materials involved, any temperature change would increase the tendency to separate. During oxidation of the anode, the increase in volume caused by the formation of the anodic oxide would likewise increase this separation tendency.

To minimize the problem of separation of the anode from the electrolyte, the anode should be in the form of a thin film since a very thin film is easily deformed and therefore follows the expansion and contraction characteristics of the ceramic substrate more easily. As the thickness of the film increases, its tendency to follow the demands of its own physical properties also increases. Therefore, as the thickness of the film increases the tendency to separate also increases. On the other hand, the anode film must be sufficiently thick to have enough metal available to provide for a significant amount of current.² The oxide formed at the anode should also be ionically

² Van Houten (19) states that a mis-match of expansion coefficients between a ceramic and a metal is permissible in the case where the metal is so thin that its elastic limit is exceeded and a permanent set takes place without unduly stressing the ceramic substrate. He indicates that metal films of 0.005 to 0.015 inches thickness are considered to be thin enough for this application.

conductive at the cell operating temperature.

Assuming that these contact problems can be solved and that the cell can be made to remain intact until the operating temperature is attained, provision must be made to insure that the anode is not appreciably oxidized chemically during the heat-up time and prior to the actual electrochemical test. A method must be devised and equipment designed such that the anodic and cathodic atmospheres might be controlled.

Electrolyte porosity is one of the properties which determines the power producing capabilities of a given cell, and therefore, presents another factor which must be considered in the design and fabrication of the cells. The electrolyte used in this work is an oxygen-ion conductor (11).³ Therefore, if the electrolyte were porous, ordinary diffusion of oxygen from the cathode to the anode would occur through the pores simultaneously with the electrochemical migration of oxygen ions through the electrolyte. The oxygen which had diffused could then combine with the anode in an ordinary chemical reaction, thus increasing the rate of anodic oxide film growth. This would

³Since the electrolyte is an oxygen-ion conductor, the half-cell reactions would of necessity be described in the following way:

Anode: Metal + oxide ions \rightarrow metal oxide + electrons.

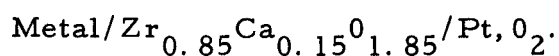
Cathode: Oxygen + electrons \rightarrow oxide ions.

Over-all reaction: Metal + oxygen \rightarrow metal oxide.

increase the rate of cell polarization and decrease the amount of electrical power available from the cell. Also, if the electrolyte were excessively porous, the anode material would diffuse through the pores in the electrolyte. This would tend to increase the electronic conductivity of the electrolyte and thus reduce the amount of power obtainable from the cell, since electronic conductivity of the electrolyte has the effect of shorting out the cell and causing it to discharge internally.

Scope of this Work

This dissertation is an account of the investigation of the feasibility of using solid calcia-stabilized zirconia as the electrolyte in a cell with a solid metallic anode and a solid-gaseous cathode at an operating temperature of approximately 1000° C. Specifically, the electrolyte composition was limited to the solid solution containing 15 mole percent calcia and 85 mole percent zirconia. The cathode consisted of a thin porous platinum electrode bonded to the electrolyte and enveloped in an oxygen-containing atmosphere. A thin film of metal deposited on the opposite face of the electrolyte was the anode. The diagrammatic representation of the cell would therefore be



Because the primary interest was in various anode materials, only

the above cathode assembly was employed. It has been studied by a number of people (for example, 11) and proven workable and simple, both in construction and operation. The anode materials investigated were iron, nickel, manganese, molybdenum, zirconium, yttrium, cobalt, chromium, and a zirconium-yttrium mixture.

The power producing capabilities of the cells operating as primary batteries were evaluated. In addition the possibility of operating the cells as secondary batteries was investigated. No attempt was made to optimize the performance or size of any cell, although data for cells, discharging through various load resistances, are presented where possible. Success in fabricating and testing complete cells was achieved only with iron, nickel, cobalt, and manganese.

LITERATURE REVIEW

A considerable amount of work has been done recently in the area of fuel cell research (1, 10). A significant number of papers published have been concerned with the use of the solid electrolyte, as employed in this work, in the development of high temperature fuel cells (3). The electrolyte has been studied extensively and the mechanism of ionic conduction is quite well understood (6, 11).

Zirconia has monoclinic symmetry at room temperature and transforms to a tetragonal form at about 1100°C accompanied by a large disruptive volume change (6). If metal oxides such as calcia or magnesia are added to the zirconia, the zirconia transforms into a cubic structure (6). With this transformation, the inversion which occurs in a pure oxide from the tetragonal high temperature form to the room temperature monoclinic form is suppressed.

Considerable disagreement exists about the cubic phase region in the ZrO_2 - CaO system. Duwez and co-workers (8) showed that zirconia compositions containing 16 to 30 mole percent calcia have cubic symmetry when quenched from 2000°C . Hund (9) found the cubic phase to exist from 10 to 20 mole percent calcia in specimens prepared at 1460°C . Dietzel and Tober (7) reported that cubic solid solutions extend from 7 to 24 mole percent calcia at 1400°C . Volchenikova (20) places the cubic phase region between 10 and 40

mole percent calcia in specimens prepared at 1500° C. However, they all agree that the cubic solid solutions in this system have a fluorite-type structure. There is also general agreement that Zr^{+4} and Ca^{+2} ions completely fill the cation sites and electrical neutrality is preserved by the creation of anion vacancies, the number of vacancies created being equal to the number of molecules of CaO added.

A number of papers have been published reporting the measurements made of the electrical conductivity of calcia-stabilized zirconia (2, 9, 11, 16, 17, 18), all of which have revealed high electrical conductivities for these solid solutions at elevated temperatures. Figure 1 (Tien's data, 17) and Figure 2 (Archer's data, 2) are presented as representative curves for the conductivity of stabilized zirconia as a function of temperature and of the concentration of the stabilizing agent.

Kingery and co-workers (11), in working with the cubic solid solution $\text{Zr}_{0.85}\text{Ca}_{0.15}\text{O}_{1.85}$, have demonstrated by means of oxygen diffusion and conductivity measurements that the transference number for the oxygen ions in this solution is approximately unity. The results of conductivity measurements performed by Weissbart and Ruka (21) indicate that the electronic conductivity is less than two percent of the total conductivity. Thus, the electrical conductivity is due essentially to the movement of oxygen ions through the anion vacancies in the cubic solid lattice.

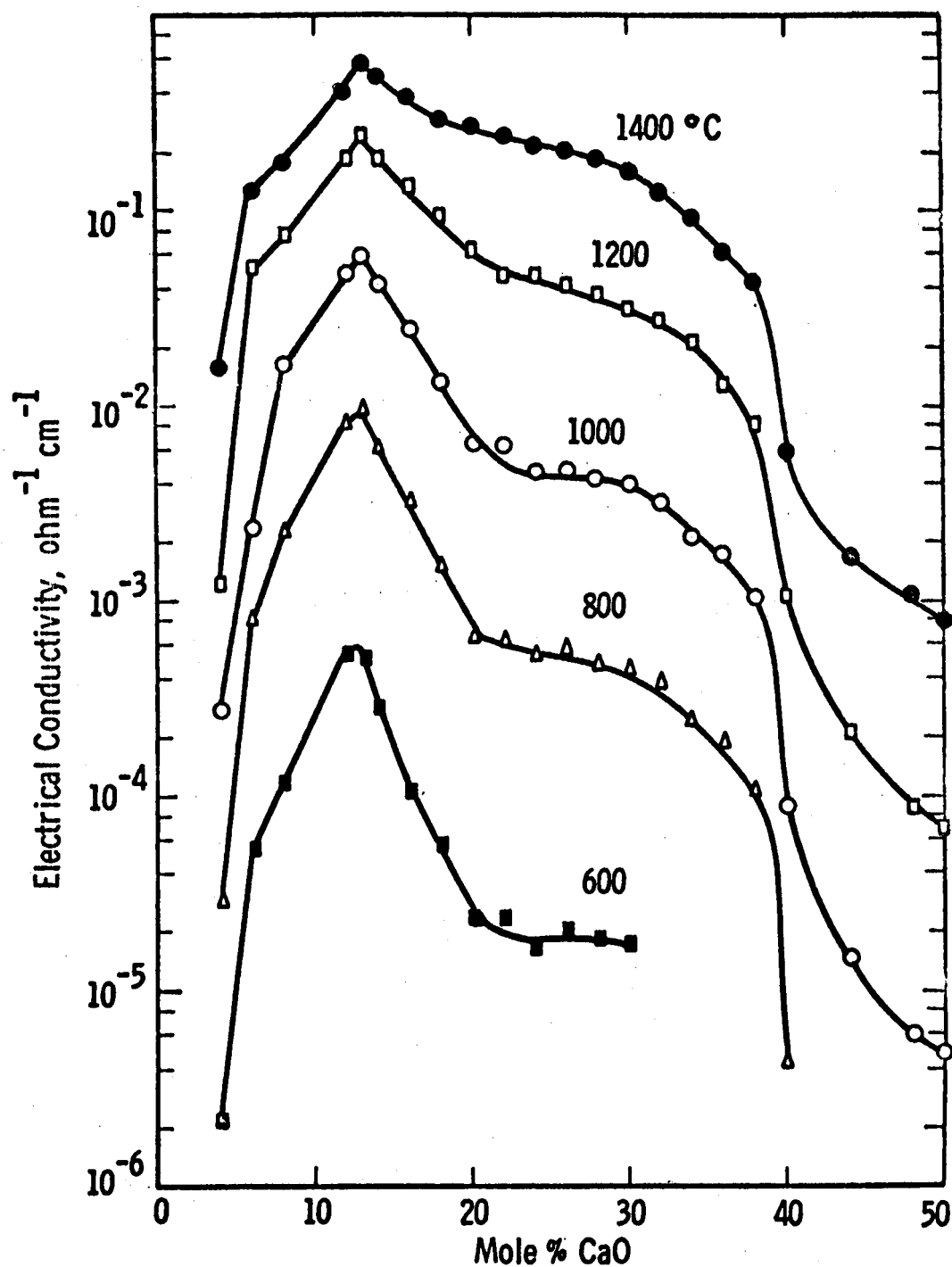


Figure 1. A reproduction of Figure 5 in the paper by Tien (17), which is a presentation of isothermal conductivity - composition data for the system $\text{ZrO}_2 - \text{CaZrO}_3$.

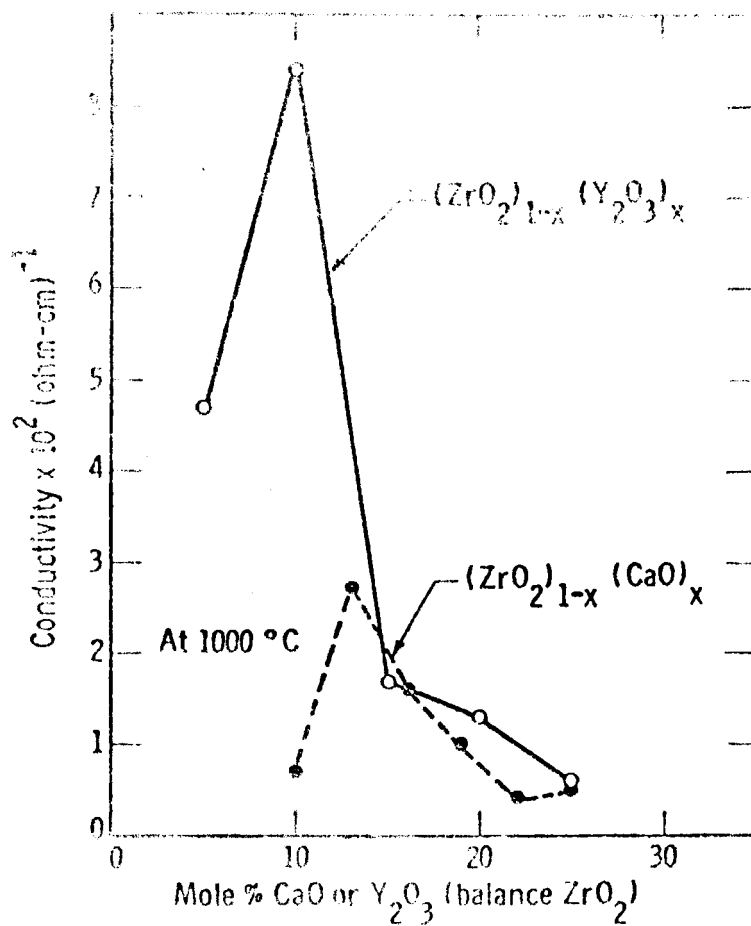


Figure 2. A reproduction of Figure 19 in a paper by Archer et al (2), which is a presentation of the conductivity at 1000° C vs. composition for $(ZrO_2)_{1-x}(CaO)_x$, where $0.1 < x < 0.25$ and $(ZrO_2)_{1-x}(Y_2O_3)_x$, where $0.05 < x < 0.25$.

Tien and Subbarao (16) have concluded that the magnitude of the ionic conductivity is controlled mainly by a compromise between the increase of conductivity due to the increased number of carriers at higher calcia compositions and a decrease in the ionic conductivity due to the decrease in mobility of the ions with increasing calcia content. They propose that since the oxygen ion must pass between two metal ions to reach an adjacent anion site the activation energy for this passage, and hence the mobility, will definitely be a function of the size of the two metal ions. Since the calcium ion is about 25 percent larger than the zirconium ion they conclude that the energy required for an oxygen ion to pass between two calcium ions will be larger than that required in passing between two zirconium ions. Their results showed an almost linear relationship between the conductivity of ZrO_2 - CaO solid solutions and composition of these solutions at various temperatures. Between 500°C and about 1100°C , the conductivity, σ , was represented by

$$\sigma = A \exp(-Q/kT)$$

where Q is the activation energy, k is the Boltzmann constant, T is the absolute temperature, and A is a constant term for each composition.

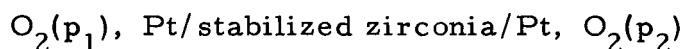
In a recent paper by Tien (16) the plots of $\log A$, activation energy Q , and electrical conductivity σ , show a maximum value for A at

about 16 mole percent calcia, a minimum activation energy at about 12 or 13 mole percent calcia, and an electrical conductivity maximum at about 13 mole percent calcia (Figure 1). For 15 mole percent calcia, Hund (9) obtained an activation energy of 1.21 electron volts while Kingery et al (11) obtained an activation energy of 1.26 electron volts.

Even though there is fair agreement in the activation energy data obtained by different experimenters, the conductivity values differ to a much greater extent. These differences have been explained by such effects as contact resistance between the stabilized zirconia and the platinum electrodes, the porosity of the specimen, and the purity of the materials used (11, 16).

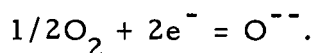
At 15 mole percent calcia (the composition of the electrolyte used in this study) the conductivity of the electrolyte is about a factor of two lower than the maximum conductivity which occurs at 13 mole percent calcia. At 15 mole percent calcia and 1000°C , the conductivity as reported by Tien (17) is approximately 3.5×10^{-2} (ohm centimeters)⁻¹.

Weissbart and Ruka (21), in their work with a hydrogen-oxygen fuel cell, constructed a vacuum tight cell of the type



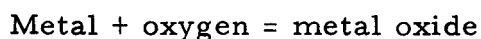
where p_1 and p_2 are the respective oxygen partial pressures. At

temperatures above 600° C the electrode reactions correspond closely to the reversible reaction



The voltages obtained were in good agreement with those calculated from the Nernst equation for an oxygen concentration cell. It was found that the electronic contribution to the total conductivity was less than 0.5 percent near 1000° C in an oxygen atmosphere.

Kiukkola and Wagner (12) have obtained high temperature thermodynamic data using galvanic cells with a stabilized zirconia electrolyte. They constructed cells consisting of a tablet of a mixture of a metal and its oxide, a tablet of the electrolyte, and a tablet of a mixture of a second metal and its oxide. These tablets were mechanically joined and placed between platinum disks connected to platinum leads. The entire cell was then placed in the furnace and was installed in such a way that the cell was under light mechanical pressure. They used this cell to obtain standard free energy changes as a function of temperature for the reaction



for metals such as cobalt, nickel, and copper.

Baur and Preis (4) probably constructed the first solid-oxide-electrolyte fuel cell. The electrolyte was in the form of a ceramic

tube which was made of 15 mole percent yttria-stabilized zirconia. The tube was filled with coke to form the anode and surrounded with iron oxide in an air atmosphere to form the cathode. An output of less than one milliamperere per square centimeter of electrolyte area was obtained at 0.65 volts and 1050° C.

Other references concerning the use of stabilized zirconia as an electrolyte in a fuel cell were concerned only with gaseous fuels and therefore were not pertinent to this work.

In summary, the papers reviewed in this section show that the mechanisms of conduction and stabilization of zirconia are quite well understood. When a foreign oxide, such as calcium oxide, is added to the zirconia, a crystal transformation takes place, and the resulting structure is cubic. This solid solution is then stable during temperature variations. The addition of the foreign oxide to the zirconia has the beneficial effect of overcoming the problem of thermal shock, and anion vacancies which are highly mobile at elevated temperatures are created by this defect state. Hence, at high temperatures the solid becomes sufficiently ionicly conductive to be used as an electrolyte. Kingery and co-workers (11) have determined the oxide ion transference number to be very close to unity and they, among others, have measured the ionic conductivity of this solid electrolyte. Tien (17) also measured the electrical conductivity of this solid and determined that the maximum conductivity occurred at a composition

corresponding to about 13 mole percent calcium oxide.

Although stabilized zirconia electrolytes are currently being used in high temperature fuel cell research (2, 3), no evidence exists to date that anyone, other than Baur and Preis (4), has made an attempt to use this electrolyte with a solid fuel.

FABRICATION OF CELLS

Cell Design

The cell design used in this investigation consisted of a simple sandwiched arrangement of the cell components. The basic component was a 15 mole percent calcia-stabilized zirconia crucible,⁴ one-inch in diameter, with walls approximately 1/16-inches thick. The cell itself was built around the base of the crucible, and the crucible form was used merely for ease of handling. The inside base was coated with a layer of porous platinum which became the cathode of the cell when immersed in an atmosphere of oxygen. The outside base of the crucible was made the anode of the cell. The metal studied was joined to the electrolyte by vapor deposition. The anode and cathode

⁴When this research was begun, the conductivity of the stabilized zirconia was reported to be a maximum at the 15 mole percent level, and the crucibles initially fabricated and purchased were of this composition. Subsequently it was reported that the maximum actually occurred at 13 mole percent calcia. However, since the research had already begun and some data had been taken, it was decided to continue with this 15 mole percent composition, at the same time being fully aware that if the higher conductivity material were used a higher current could be drawn from the cell at the same voltage. However, the discharge curve would have the same general shape. The only difference would be the increase of the current due to the lower internal resistance in the case of the 13 mole percent electrolyte. The crucibles were supplied by Zirconium Corporation of America, Solon, Ohio, and U. S. Bureau of Mines, Albany, Oregon.

were then connected, via platinum lead wires, to the recording instruments outside the furnace.

Cell Construction

The crucibles used in this work exhibited a slight curvature across the base. Hence, before any work was done with the crucible, it was necessary to grind the base of the crucible flat. This was accomplished by rubbing the base of the crucible across emery cloth (silicon carbide) which was supported on a hard flat surface. The grinding was continued until no curvature could be visually detected. Coarse paper was used to effect faster grinding and to leave the electrolyte with a rough surface. This roughness should have the effect of increasing the area available for the electrode reaction and of helping to promote more effective bonding between the electrode and the electrolyte. After this initial grinding the crucible was thoroughly cleaned and the first coat of platinum paste⁵ applied.

The inside base of the crucible was coated with two layers of platinum paste, each fired separately at approximately 1000° C for one hour. It was found that a two-coat application was necessary in order to have an electrode which was thick enough for good conduction and also to maintain intimate electrode-electrolyte contact. If one

⁵ No. 6082, Englehard Industries Incorporated, Newark, New Jersey.

thick coat was applied the platinum electrode separated excessively from the electrolyte.

Early work with vapor deposition of the anode material showed that some monitoring technique was necessary to determine the extent of deposition. The method developed⁶ required the use of small platinum electrodes on the outside base of the crucible. Consequently, small bits of platinum paste were painted on opposite sides of the base of the crucible at the same time that the cathode platinum was applied. It was found that two layers of platinum were sufficient for both the cathode and the small monitoring electrodes on the anode side of the cell.

The fabrication of the anode presented difficulties of a greater magnitude. Early in the investigation it was concluded that the best method available for applying the anode film to the electrolyte was vapor deposition of the anodic material in a vacuum (considering the equipment and funds available for this project). It was thus necessary to construct a vacuum system capable of maintaining a dynamic vacuum of about 10^{-5} Torr.⁷ A vacuum system with capabilities

⁶ Because the electrical resistance through the film between the two monitoring electrodes is directly related to the thickness of the film, the extent of the deposition was determined merely by measuring this resistance with an ohmmeter.

⁷ One Torr equals one millimeter of mercury.

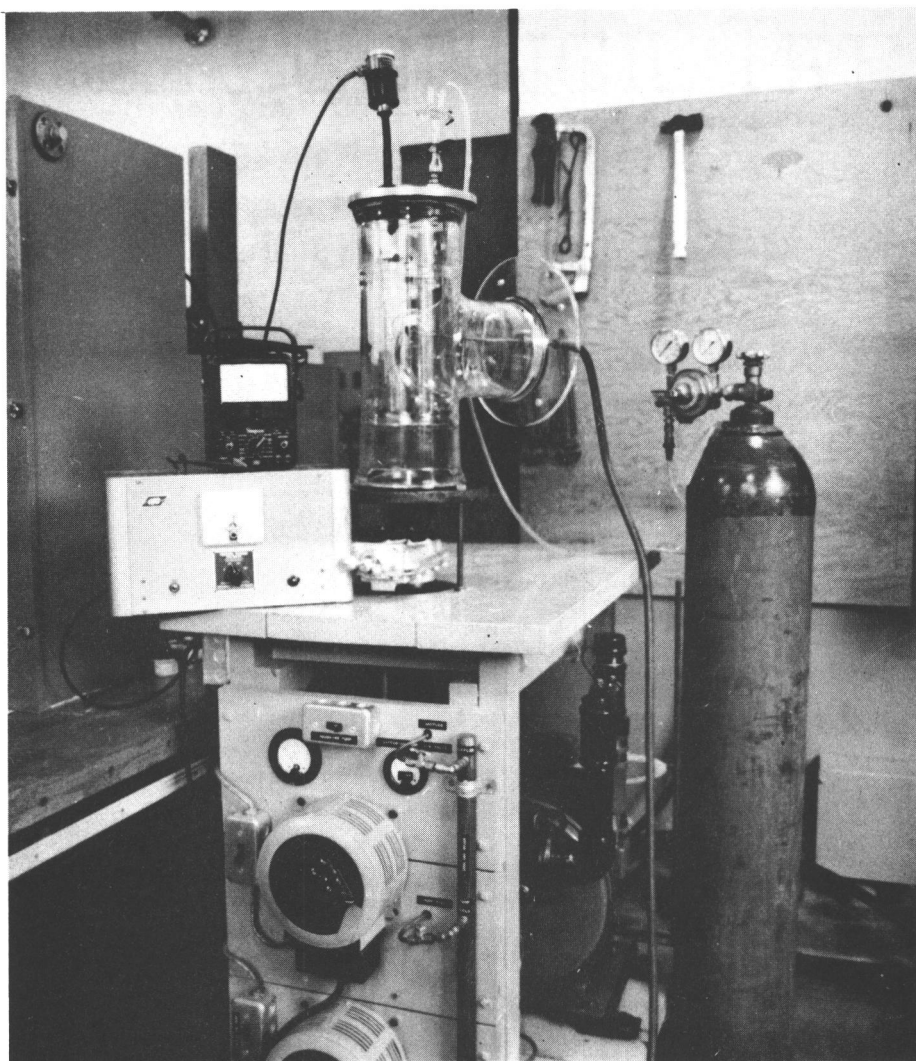


Fig. 3. Photograph of the assembled vacuum equipment. (See page 23 for construction details)

theoretically exceeding this specification was built using a Welch Duo-Seal high vacuum two-stage roughing pump,⁸ a four-inch oil diffusion pump,⁹ and a six-inch Pyrex glass tee with O-ring seals as the vacuum chamber. Auxiliary supporting equipment included a Phillips vacuum gauge and tube,¹⁰ a one-and-one-half-inch vacuum valve, electrical leads and the necessary supporting electrical equipment. Figure 3 is a photograph of the assembled equipment. The entire vacuum system was tested with a mass spectrometer helium leak detector.¹¹ The system was leak free to within the sensitivity of the detector. The vacuum attainable was approximately 2×10^{-6} Torr. (The pressure in the system during the vapor deposition process was approximately 5×10^{-5} Torr.)

The first experiments in the vapor deposition work were with chromium. Chromium metal was melted onto a tungsten basket filament¹² in a helium atmosphere to insure good thermal contact between

⁸Serial no. 1840-97, W. M. Welch Manufacturing Company, Chicago, Illinois.

⁹Model MC-275-01, Distillation Products Incorporated, Rochester, New York.

¹⁰Type PHG-09, Consolidated Vacuum Corporation, Rochester, New York.

¹¹Model MS-9, Veeco Vacuum Corporation.

¹²All filaments used in the vapor deposition experiments were supplied by the R. D. Mathis Company, Long Beach, California.

the chromium and the tungsten filament. The filament was then connected to electrical leads and heated resistively to the operating temperature required for deposition. An optical pyrometer¹³ was used to measure the temperature of the filament. The coatings obtained on the clean ceramic substrate were adherent but were far too thin to be used for any further experimentation. The resistance across the base of the crucible through this metallic film was always greater than about 1000 ohms, which indicated that the film was not thick enough for use in a cell. This failure to obtain a sufficiently thick coating led to the introduction of the previously mentioned monitoring technique.

Copper leads were connected by spring-loaded contacts to the small platinum monitoring electrodes on the base of the crucible. These leads were then connected to an ohmmeter¹⁴ outside the vacuum chamber. This set-up made it possible to monitor the deposition process by measuring the resistance across the deposited film on the base of the crucible. The electrical power to the tungsten filament was increased just enough to move the ohmmeter needle which showed that deposition was occurring. The deposition process was continued until the resistance was 15 to 20 ohms. With some

¹³ Leeds and Northrup Company, Philadelphia, Pennsylvania.

¹⁴ Simpson 270 VOM, Simpson Electric Company, Chicago, Illinois.

metals this required more than one filament. The cell was then removed from the vacuum chamber and leads were connected to the spring-loaded contacts and additional metal was deposited on the base of the crucible using common electroplating techniques. This process was continued until the film was approximately 0.001 to 0.002 inches thick. (See Appendix II for specific details pertaining to each metal used.) The anodic materials selected for this study were iron, nickel, manganese, cobalt, molybdenum, zirconium, yttrium, and chromium. (See Selection of Anodes, Appendix I.)

EXPERIMENTAL PROCEDURE FOR CELL TESTING

To test the cells as described in the previous section, the equipment used must satisfy the following requirements:

1. The furnace must be capable of operating continuously at a temperature of at least 1000° C.
2. The control mechanism for the furnace must be able to maintain the temperature constant at some preselected value.
3. Provision must be made to transport an oxygen-containing atmosphere to the cathode compartment in such a way that this atmosphere will be forced to flow across the platinum electrode.
4. An inert atmosphere must be maintained in the anode compartment to prevent chemical oxidation of the anode.
5. Supporting electrical equipment must be provided. This would include voltage and current measuring and recording devices, flowmeters and valves for control and measurement of the gases involved, a variable load resistor, and a d-c power supply for recharging the cells after discharge.

These requirements were satisfactorily met by using the following equipment:

1. A Hevi-Duty combustion tube furnace with a maximum tube diameter of two inches and capable of continuous operation

at 1400° C.¹⁵

2. A two-inch diameter mullite work tube.¹⁶
3. A three-quarter-inch diameter 15 mole percent calcia-stabilized zirconia tube.¹⁷
4. Two universal refractory tube seals with Viton gaskets.¹⁸
5. One-quarter-inch and one-eighth-inch diameter alumina tubes.¹⁹
6. Swagelok tube fittings with Teflon ferrules.²⁰
7. A type-K chromel-alumel thermocouple.
8. Honeywell Pyr-O-Volt proportional controller with magnetic amplifier and saturable core reactor.²¹

¹⁵Type G-02712-PT, Hevi-Duty Electric Company, Milwaukee, Wisconsin.

¹⁶McDanel Refractory Porcelain Company, Beaver Falls, Pennsylvania.

¹⁷Zirconium Corporation of America, Solon, Ohio.

¹⁸McDanel Refractory Porcelain Company, Beaver Falls, Pennsylvania.

¹⁹Ibid.

²⁰Crawford Fitting Company, Cleveland, Ohio.

²¹Model 105R12 with Model 6191 Brown amplifier, Minneapolis Honeywell Regulator Company, Philadelphia, Pennsylvania.

9. A zero to ten thousand ohm variable resistor.
10. A zero to one thousand ohm variable resistor.
11. A two channel strip chart recorder.²²
12. Flexible Tygon tubing, one-quarter-inch diameter.
13. One-and-one-half volt ignition dry cells.
14. Tip jacks connected in parallel to provide multiple electrical connections to the cell.
15. Gas control needle valves.
16. Manometer and orifice gas flow meters.
17. Molecular sieve gas drying tubes.
18. Platinum lead wires and platinum screen current collectors.
19. Cylinders of Argon and Oxygen with regulators.
20. Alundum refractory cement and Sauereisen thinning liquid.

A photograph of a crucible cell, ready to be tested, is shown in Figure 4, and a sectional sketch is shown in Figure 5. The cell is attached to the zirconia tube (Figure 5) by slipping the sides of the crucible (A)²³ over the outside of the tube (B) and cementing this joint with alundum cement moistened with Sauereisen thinning liquid (C). The cement is allowed to dry for about 10 hours. The assembly is

²²Servo-riter recorder, Texas Instruments Incorporated, Houston, Texas.

²³Capital letters refer to designations in Figure 5.

next placed inside the mullite tube in the region of the hot zone of the furnace.

Figure 6 is a sectional sketch showing the cell assembly inside the furnace. The cathodic atmosphere is transported to the cell from the gas control equipment through Tygon tubing. The Tygon tubing is attached to the one-quarter-inch alumina tube (²⁴a, D), which is inserted into the cathodic chamber inside the zirconia tube (b, B). The end of this alumina tube is covered with the platinum screen (E) used for a current collector and the platinum lead wire (F) is attached to this screen and brought outside the furnace through the alumina tube. The anodic atmosphere is transported in a similar manner to the anode chamber (c, K). The ends of the tubes which extend inside the mullite work tube are held in place by Lava²⁵ radiation shields (d) which are positioned in such a way as to effectively extend the end walls of the furnace through the tubing. A universal refractory tube seal (AA)²⁶ is placed at each end of the mullite work tube. These seals were drilled and tapped, and Swagelok O-Ring tube fittings were attached.

Figure 7 illustrates the types of fittings used on the one end of the system. A similar arrangement was used for passing two alumina

²⁴Lower case letters refer to designations in Figure 6.

²⁵American Lava Corporation, Chattanooga, Tennessee.

²⁶Double capital letters refer to designations in Figure 7.

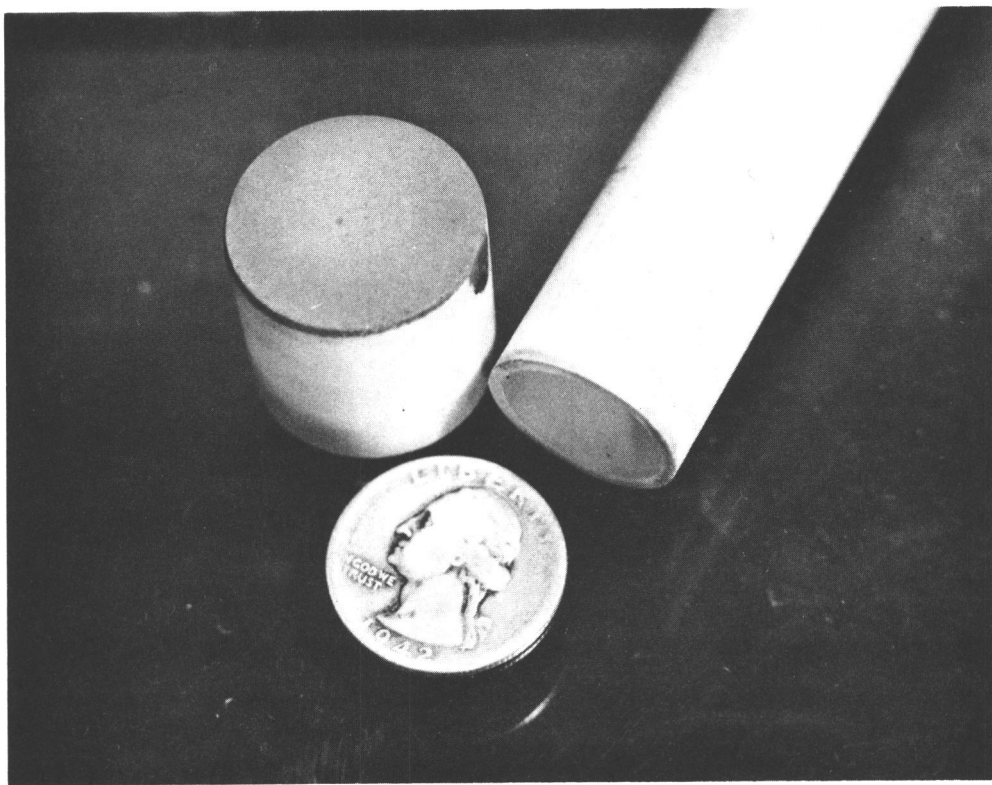


Fig. 4. Photograph of crucible cell ready for testing. Pictured also is the end of the stabilized zirconia work tube. One of the monitoring electrodes can be seen on the right side of the crucible.

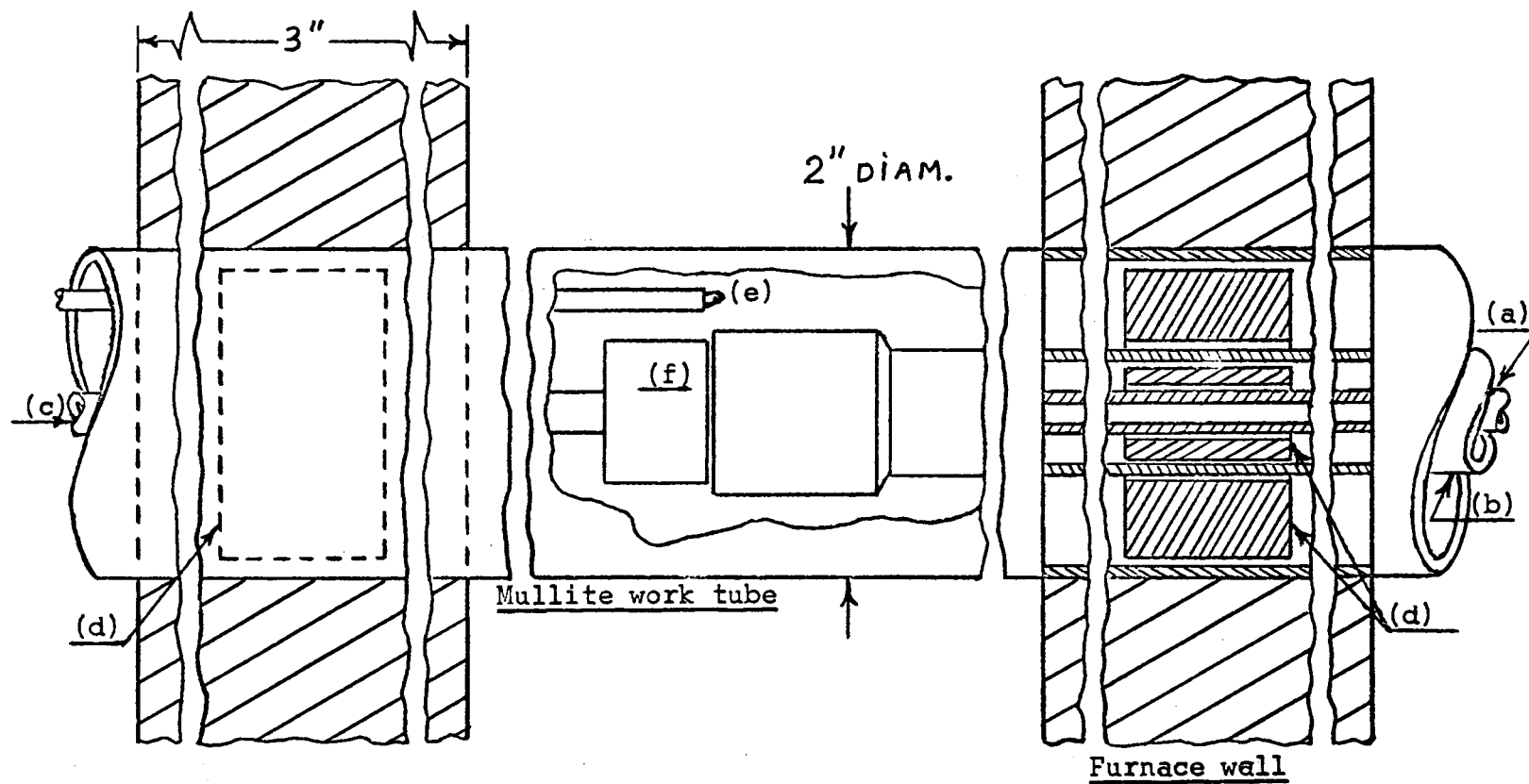


Fig. 6. Sectional sketch showing cell assembly inside of the furnace.
(See page 29 for construction details.)

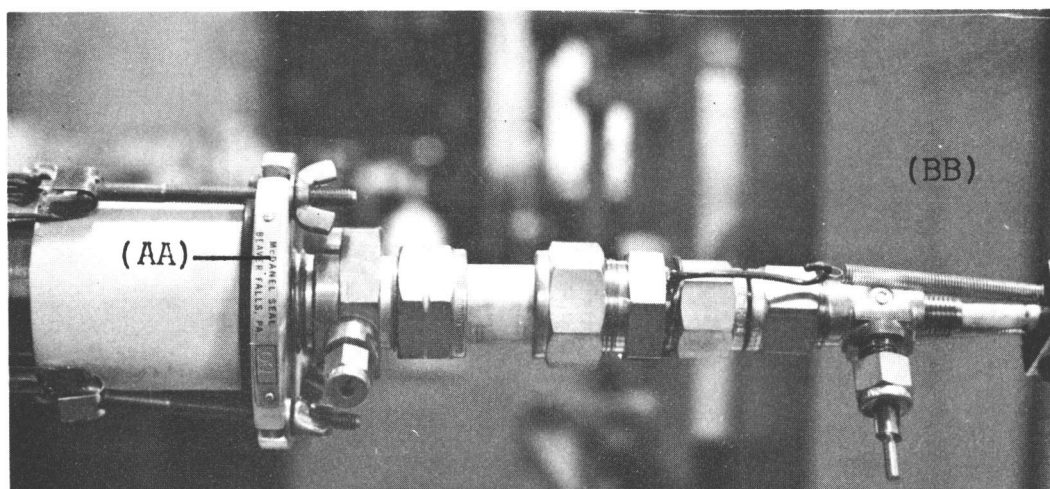
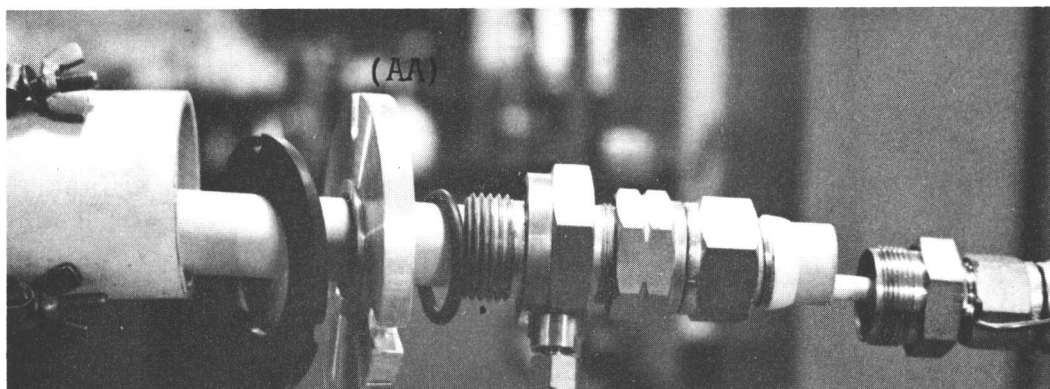


Fig. 7. Photographs showing the arrangement of the refractory tube seal and Swagelok fittings on one end of the system. Visible also are the mullite and stabilized zirconia work tubes, and the spring-loaded clamp on the small alumina tube.

tubes through the seal on the other end. (One tube was used to transport the anodic atmosphere (c) and the other tube was used to contain the thermocouple lead wires (e).) By using O-ring fittings, plus Teflon ferrules in all fittings, the cathodic and anodic atmospheres were maintained.

A block of Lava (f, H) was fitted to the alumina tube used to transport the anodic atmosphere to the cell. This in turn was covered with platinum foil or platinum screen (J) which was pressed against the anode and used as a current collector. The collector was connected to a platinum lead wire extending through the alumina tube to the outside of the furnace. Both anode and cathode electrical contacts were maintained by using spring-loaded clamps (BB) on the alumina tubes, forcing the platinum collectors against the electrodes and holding them there with a slight pressure during the entire testing operation.

The chromel-alumel thermocouple (e, G) which was connected to the Pyr-O-Volt controller, was positioned adjacent to the cell itself inside the mullite tube, but outside the zirconia tube. This thermocouple was used to control the temperature as well as to indicate the temperature of the cell. The Pyr-O-Volt proportional controller was capable of maintaining the temperature inside the furnace to within a few degrees of the desired operating temperature, usually 1000° C.

For all of the cells tested, argon was used as the anode

atmosphere and a mixture of argon and oxygen was used as the cathode atmosphere. The gases were transported from the high pressure storage bottles through Tygon tubing to the manometer and orifice gas flow meters. The orifices were made by drawing ten-millimeter glass tubes down to filaments which were mounted within another glass tube for protection. The flowmeter system was then calibrated so that, if necessary, calculations could subsequently be made to determine the composition of the cathodic atmosphere. The gases flowed from this measuring system through the molecular-sieve drying tubes to the cathode and anode chambers.

The platinum lead wires were connected via tip jacks to copper wires, which were in turn connected to the terminal board constructed for this purpose (Figure 8). Figure 9 shows the electrical circuit used for the measurement of the voltage and current of the cell. The ten-thousand-ohm variable resistor²⁷ was used as the load resistance (E)²⁸, and the one-thousand-ohm variable resistor²⁹ was used as a shunt resistance (D) to measure the current through the cell. Channel A of the strip chart recorder was used for the voltage of the cell and

²⁷Decade resistor, Leeds and Northrup Company, Philadelphia, Pennsylvania.

²⁸Letters refer to designations of Figure 9.

²⁹op. cit.

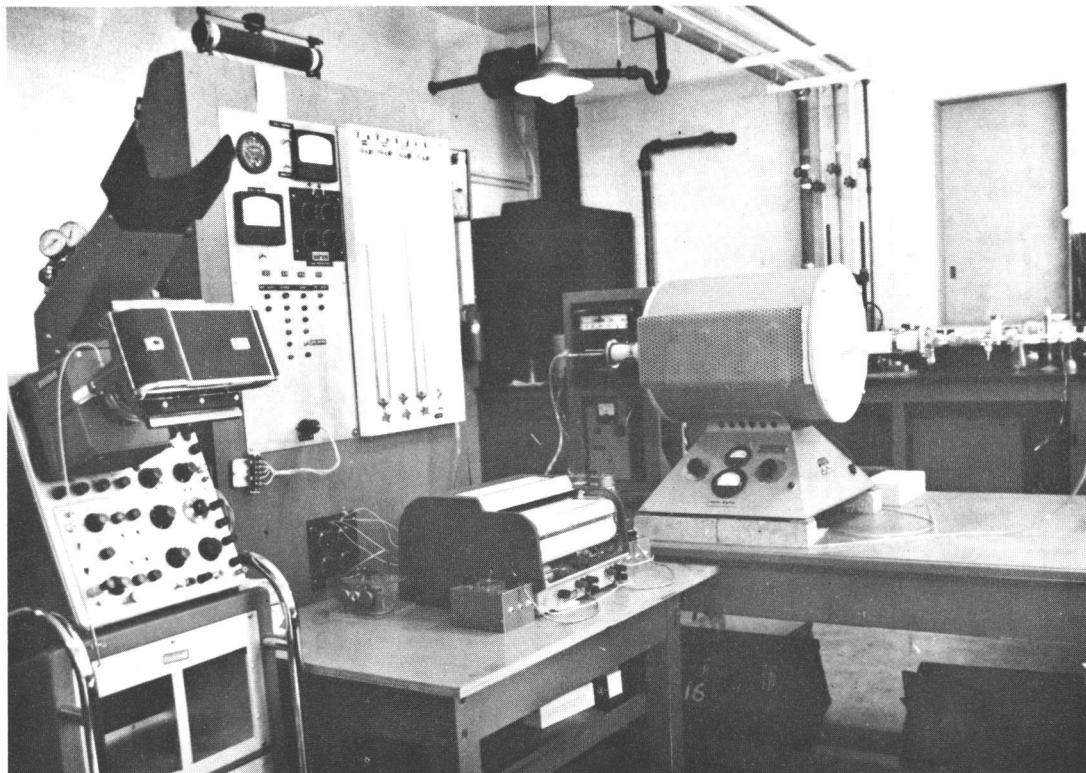


Fig. 8. Photograph of the equipment used for cell testing. Visible are the tube furnace with tube assembly, two-channel recorder, terminal board, and oscilloscope with camera attachment.

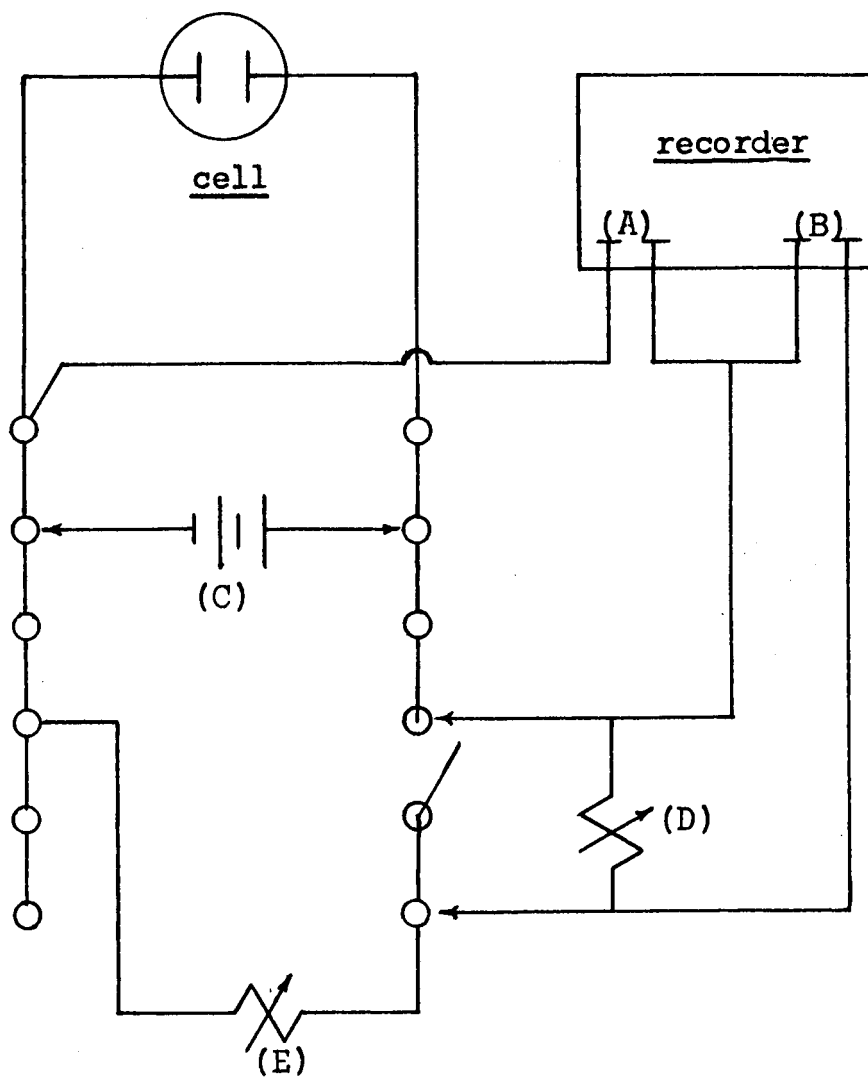


Fig. 9. Circuit diagram for cell testing.

channel B recorded the current through the cell.

With the cell and supporting equipment completely assembled, the furnace was turned on and allowed to heat up to 1000° C. The heat-up time was generally two to three hours. During this initial heat-up period, a d-c current source (C) was connected to the cell in such a way as to oppose the EMF of the cell. This back-EMF was applied solely to help prevent any premature chemical oxidation of the anode. When the temperature reached 1000° C the back-EMF was removed and the cell performance was recorded. At the end of the discharge run, this back-EMF was again applied in an attempt to recharge the cell. The open circuit voltage of the cells was checked occasionally with a K-2 potentiometer,³⁰ and this value was compared to, and found to be in close agreement with, the voltage indicated by the recorder.

³⁰ Leeds and Northrup Company, Philadelphia, Pennsylvania.

EXPERIMENTAL RESULTS

The discharge characteristics of the cells investigated are shown on Figures 10-18. The curves were obtained by successively charging and discharging the cells tested. Cell potential-time (even numbered figures) and cell current-time (odd numbered figures) characteristics are shown for iron, nickel, manganese and cobalt. (See Appendix II for a discussion of the anode materials tried and for the reasons why success in fabricating workable cells was achieved only in the case of the above four metals.) The numbers adjacent to each curve are the nominal values of the load resistance, in ohms, through which the cells were discharged.

Figure 18 is representative of the reproducibility of these data. It shows curves obtained during the discharge of two different iron cells and two different nickel cells discharging under the same conditions (3 ohms load, 1000° C). The results in both cases were in satisfactory agreement, showing the reproducibility of the experimental procedures employed. Only one cell was constructed and tested for each of the remaining anode materials--manganese and cobalt.

Table I gives the energy produced by each cell tested plus a comparison of the measured open-circuit potential with the theoretical EMF for each cell. The energy was computed by a graphical

evaluation of the expression

$$\text{energy} = \int_0^{t_f} (EI) dt$$

where E is the cell potential, I is the cell current, t is the time, and t_f is the total discharge time. For the iron, nickel, and cobalt cells, zero time was taken to be the point where the flat portion of the curve began, immediately after the initial prominence of the curve. Since this initial prominence was absent from the manganese curves, the actual zero of time was used in this case for the cell discharge. Justification for this action is established in the Discussion of Results.

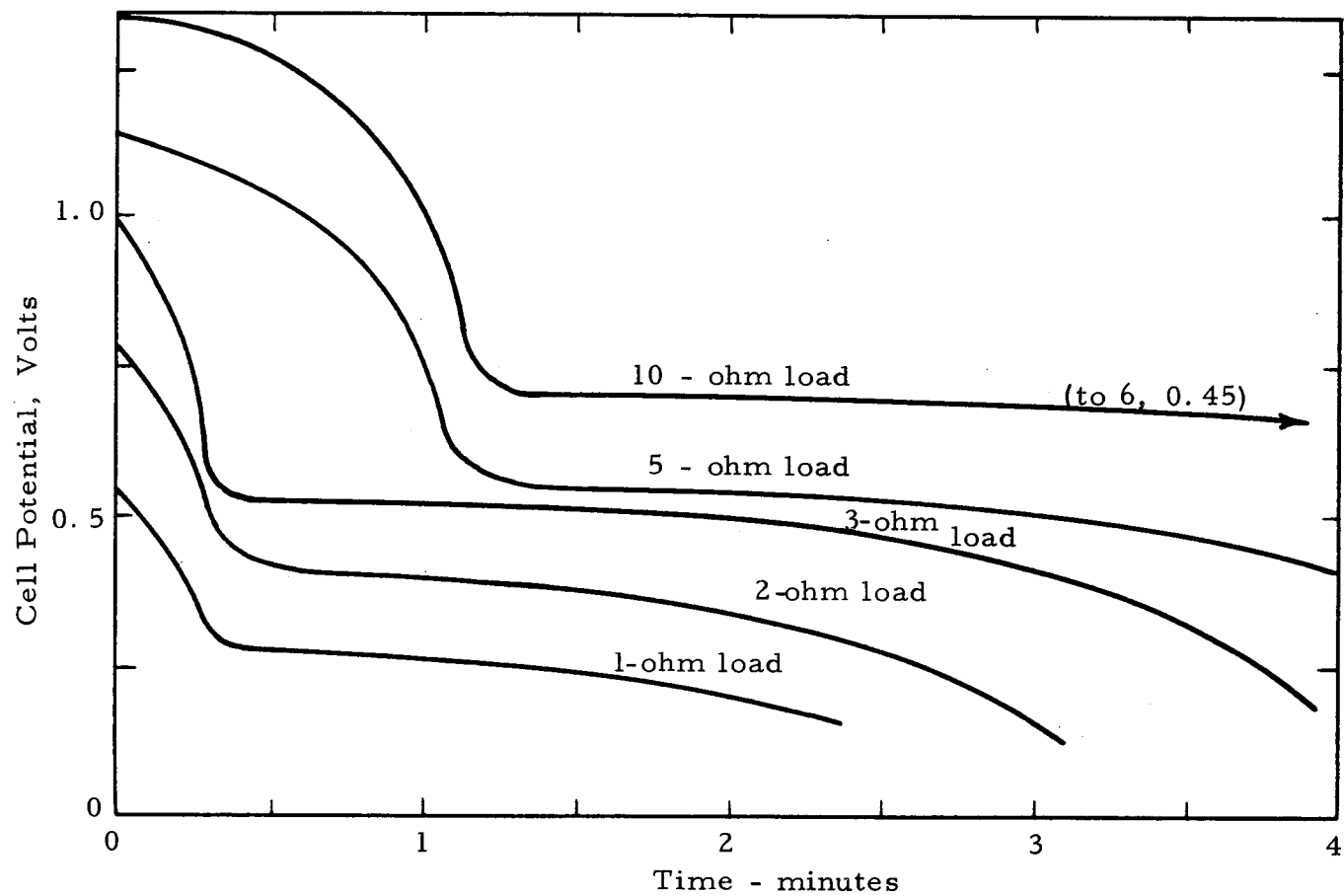


Figure 10. Discharge curves for the cell Fe/Stab. Zirc./Pt, O₂.

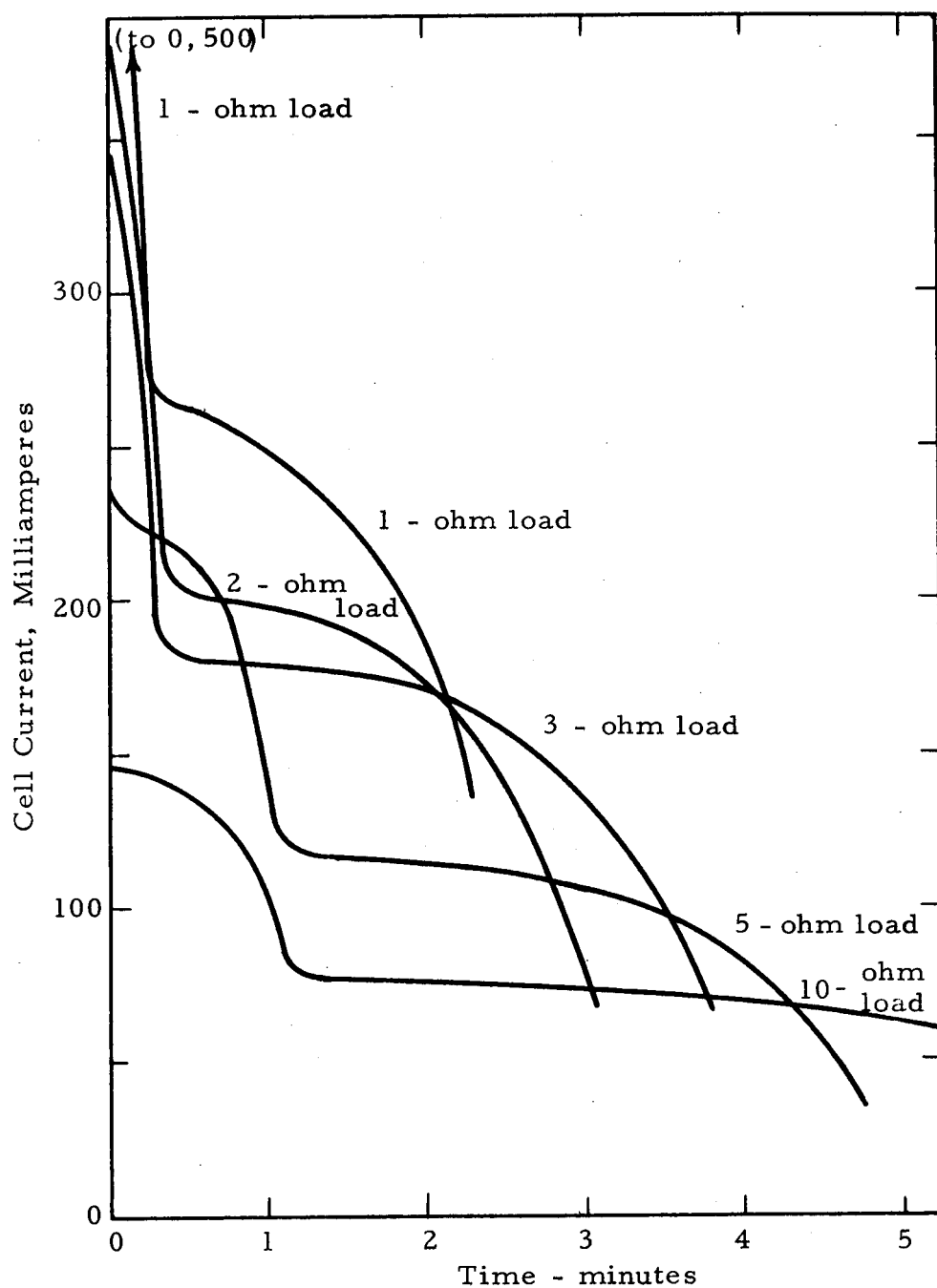


Figure 11. Discharge curves for the cell Fe/Stab. Zirc./Pt, O₂.

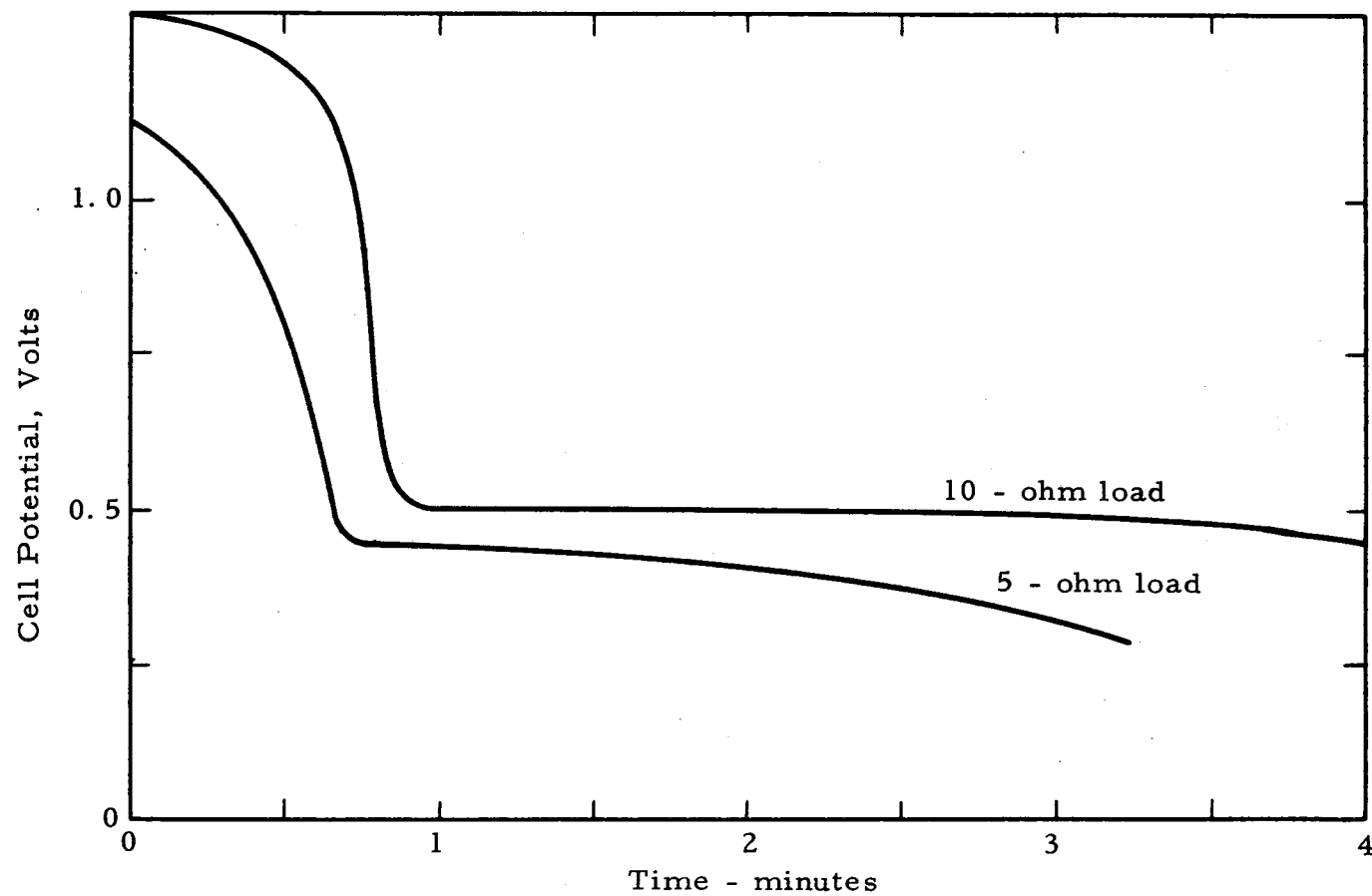


Figure 12. Discharge curves for the cell Ni/Stab. Zirc./Pt, O₂.

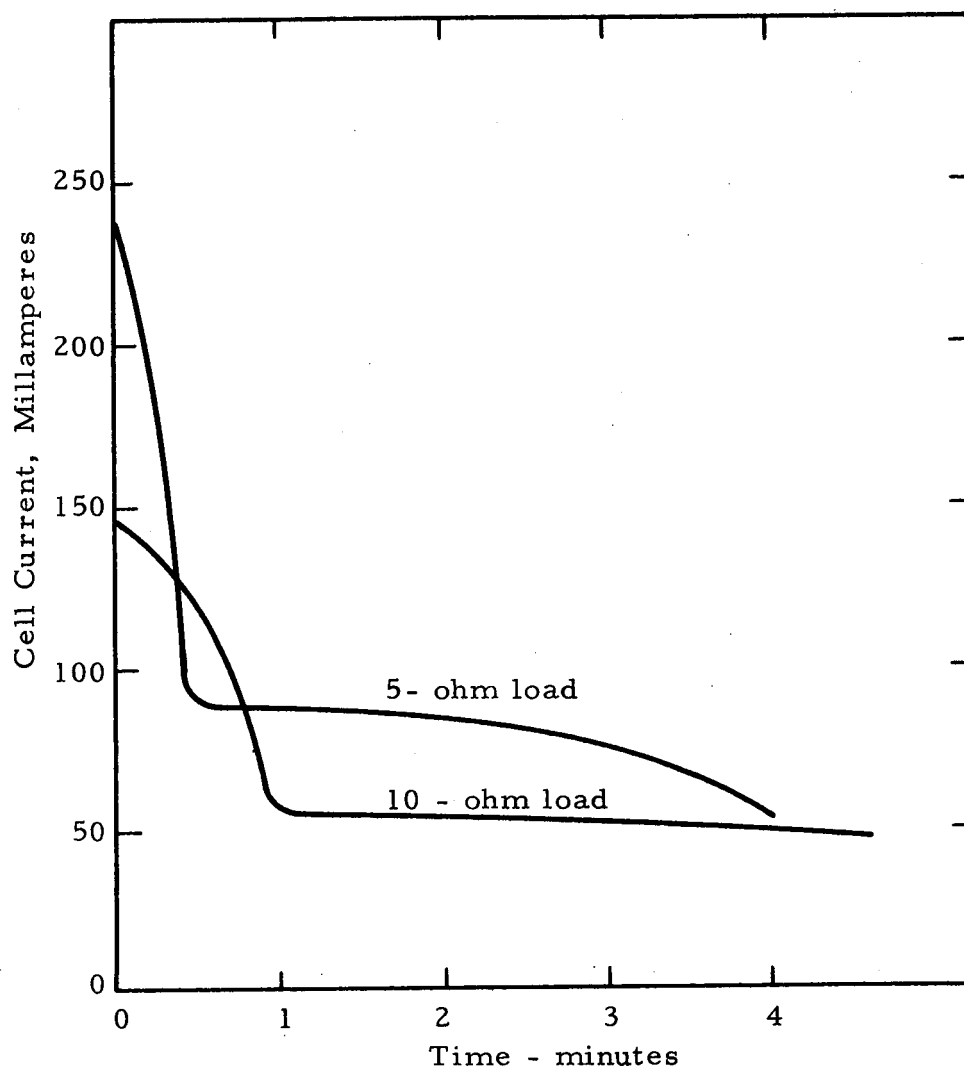


Figure 13. Discharge curves for the cell Ni/Stab.
Zirc. /Pt, O₂.

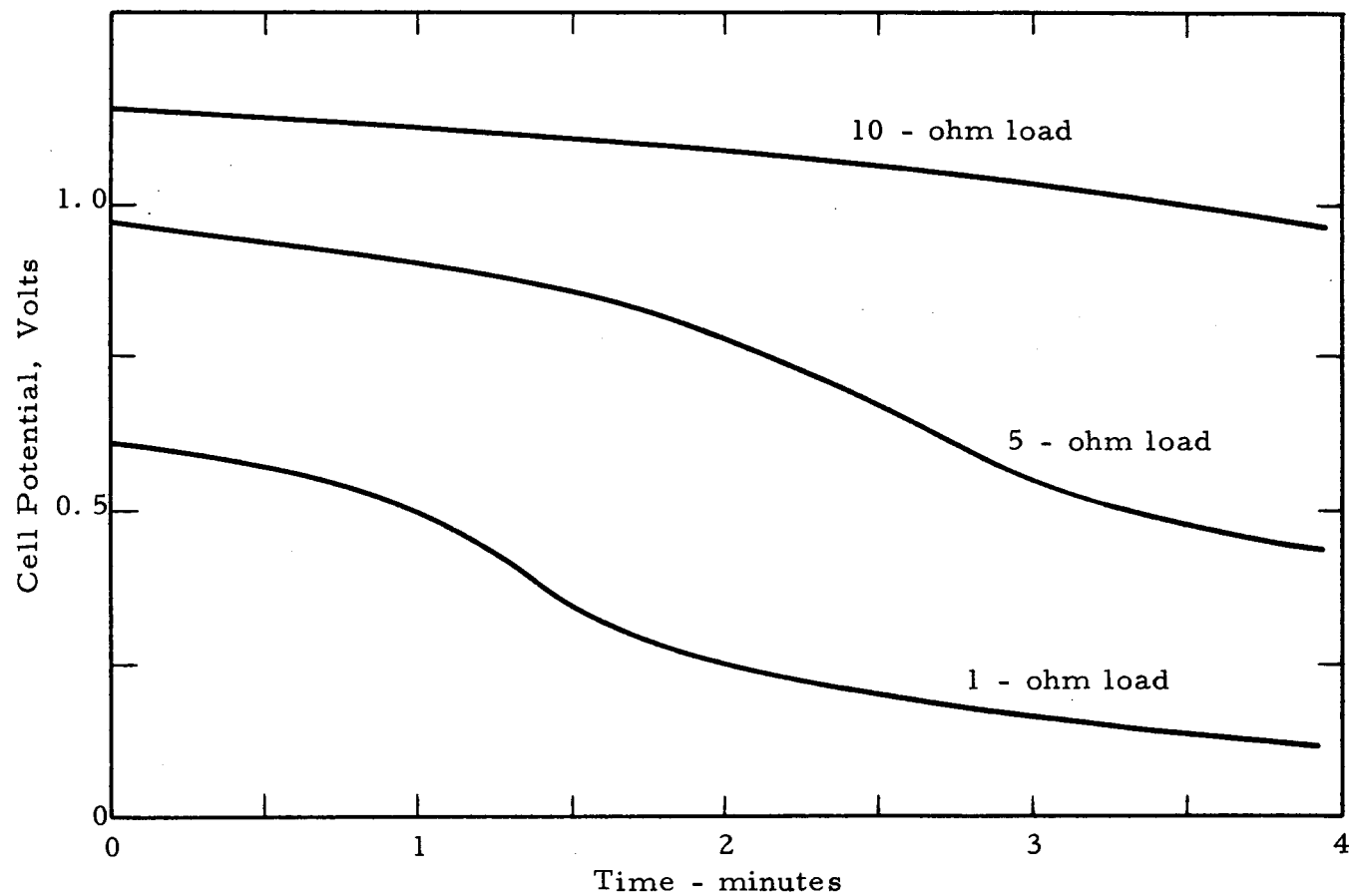


Figure 14. Discharge curves for the cell Mn/Stab. Zirc. /Pt, O₂.

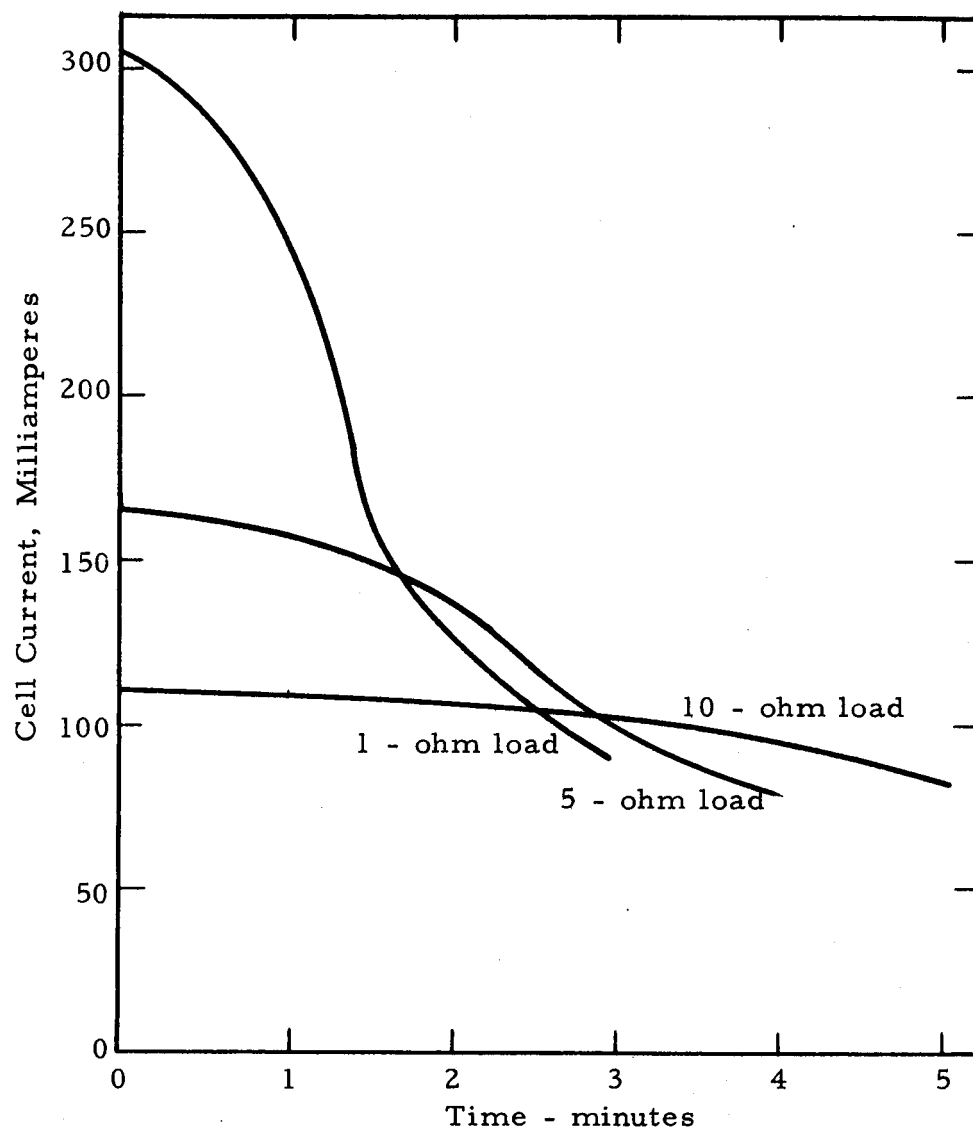


Figure 15. Discharge curves for the cell Mn/Stab. Zirc. / Pt, O₂.

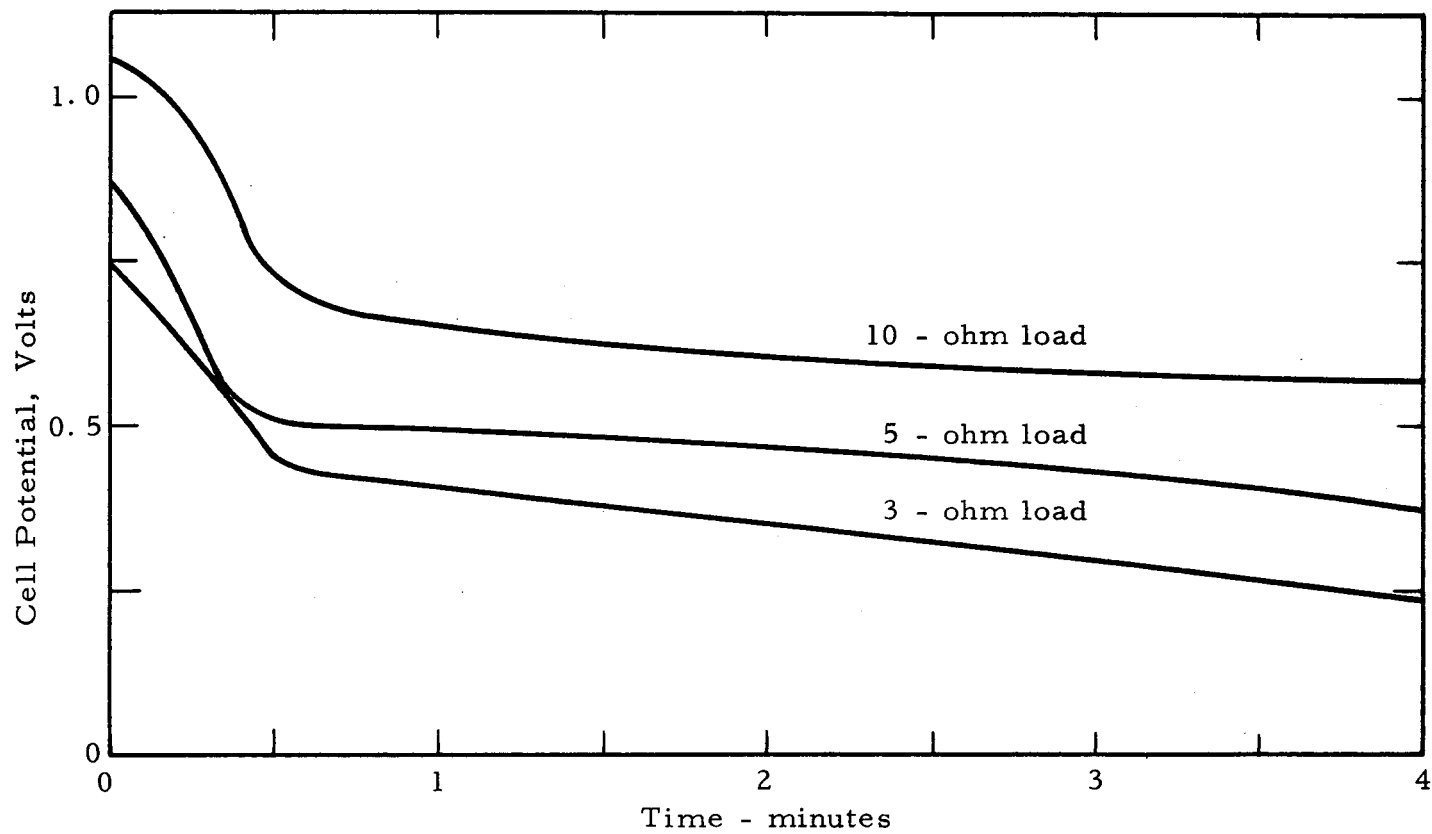


Figure 16. Discharge curves for the cell Co/Stab. Zirc./Pt, O₂.

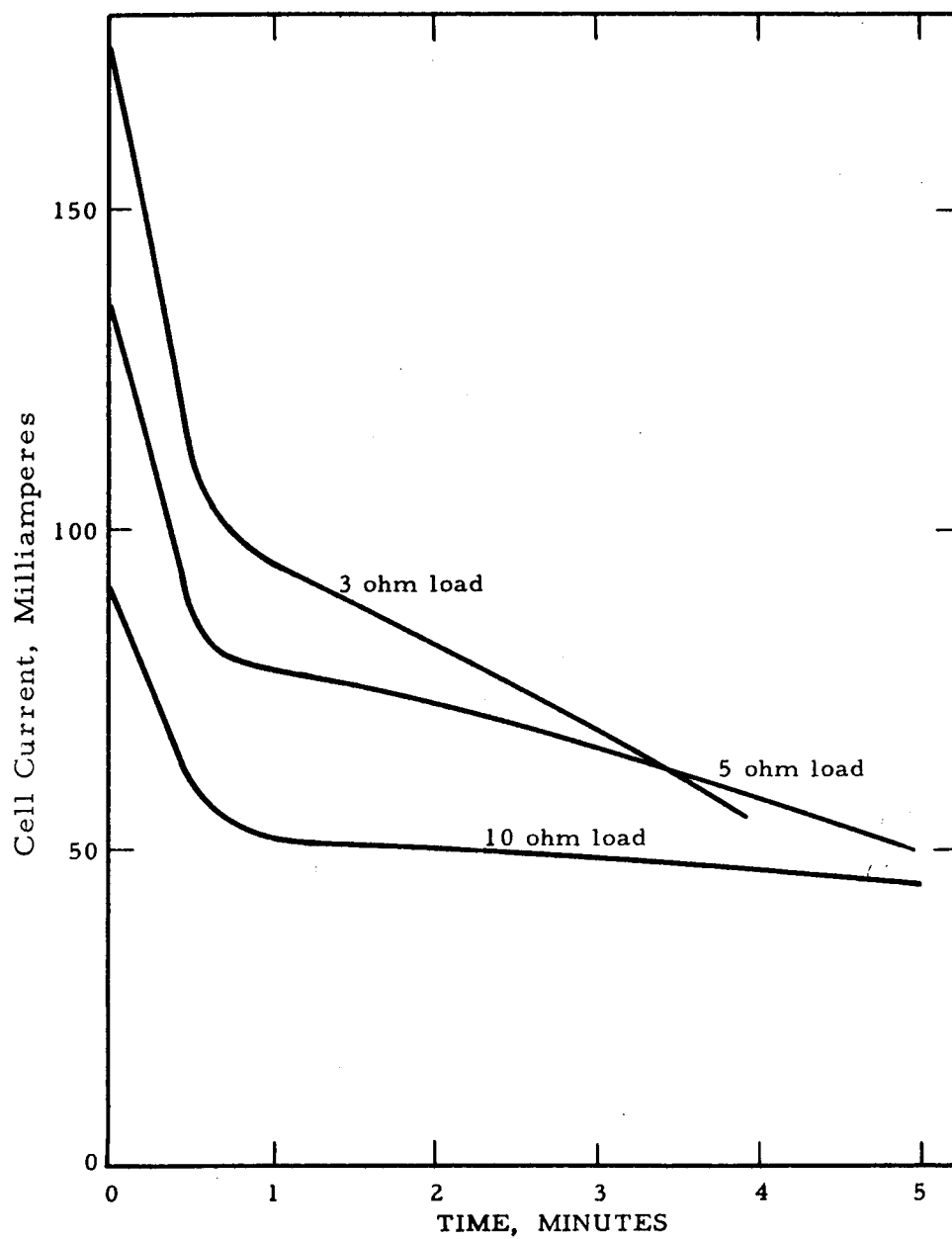


Figure 17. Discharge curves for the cell Co/Stab. Zirc/Pt, O₂.

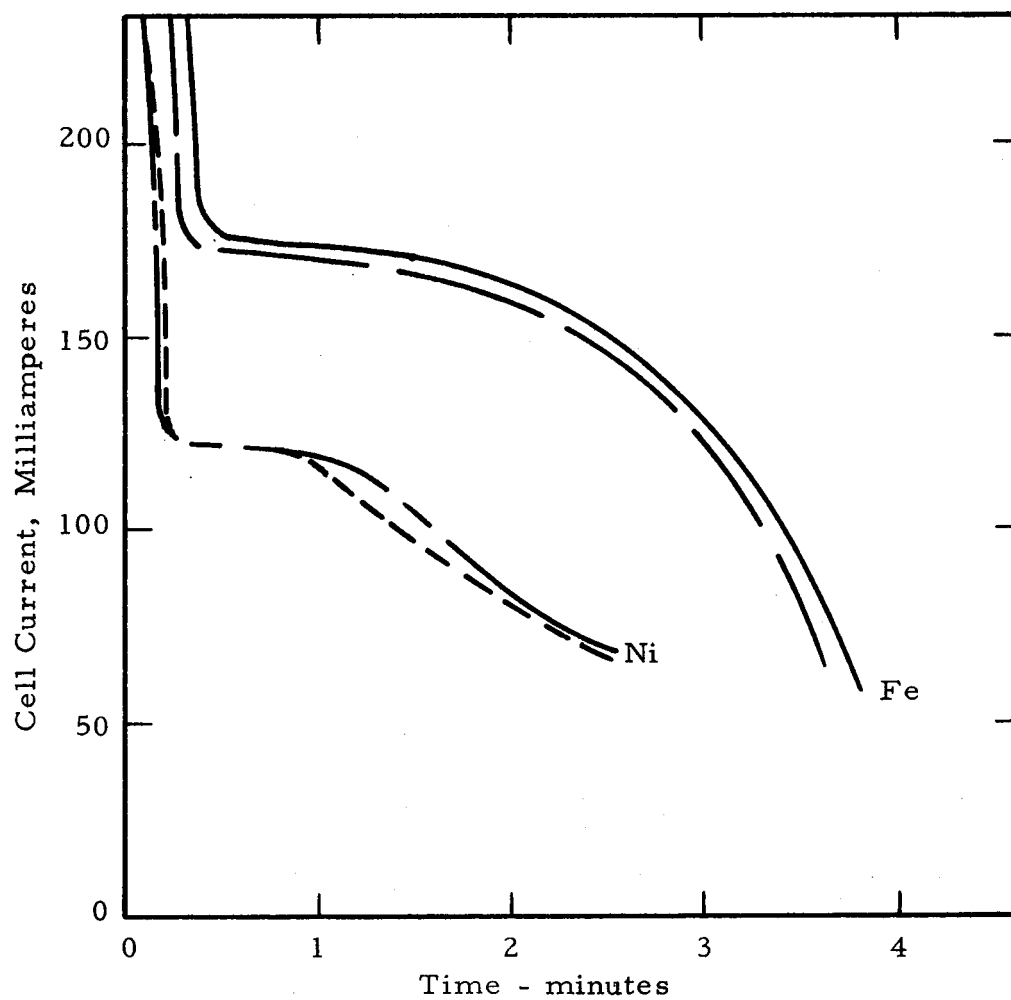


Figure 18. Reproducibility of data for iron and nickel anodes discharged through a fixed resistance.

TABLE I. ENERGY OUTPUT AND OPEN CIRCUIT POTENTIAL OF EACH CELL TESTED.

Cell anode	Nominal load, ohms	Energy density, watt-hrs/ft ³ *	Discharge time, minutes**	Theoret. EMF, volts (22)	Open circuit pot. , volts***
iron	5	138.4	3.5	0.857, 0.923, 0.928	0.90 - 0.91
iron	10	145.5	4	0.857, 0.923, 0.928	0.90 - 0.91
iron	10	127.4	3.5	0.857, 0.923, 0.928	0.90 - 0.91
nickel	5	70.7	3.5	0.65	0.64 - 0.65
nickel	10	70.5	4	0.65	0.64 - 0.65
manganese	5	324.3	4.5	1.05, 1.22, 1.51	1.34 - 1.51
manganese	10	397.8	5	1.05, 1.22, 1.51	1.34 - 1.51
cobalt	5	95.7	4.5	0.55 - 0.75	0.74 - 0.84
cobalt	10	119.2	6.25	0.55 - 0.75	0.74 near the end of the discharge

*Volume was actual cell volume (approximate cell dimensions: 1"D. x 0.045" thick for Fe; 1"D. x 0.050" thick for Ni, Mn, Co).

**Discharge time was from the end of the initial prominence to the end of the discharge cycle.

***In the case of iron, cobalt, and nickel, the open circuit potentials were measured within one minute after the decay of the initial prominence. For manganese, the measurement was taken one minute after discharge began.

DISCUSSION OF RESULTS

The cells could be recharged a number of times, as evidenced by Figures 10 through 17; therefore, they can be classified as secondary batteries.

The iron, cobalt, and nickel discharge curves have the same general shape and the discussion of these curves has been divided into two sections: (1) the flat section, and (2) the initial prominence.

The Flat Section of the Discharge Curves

The flat section of the curves is what one would expect to obtain for a battery discharging through a fixed resistance. That is, one would expect a gradual decay of the voltage and current with time. This decay would be even more pronounced if the anodic reaction products were not removed during discharge and were not ionically conductive. As will be shown later, this flat section represents the actual discharge of the anode except for the manganese cell.

It was during the discharge, as represented by this flat section, that the open-circuit potentials were measured. In the case of nickel, where only one oxide is possible, the agreement of the open-circuit potential with the theoretical EMF was very good and demonstrated the value of this type of cell as a research tool for determining thermodynamic data at elevated temperatures. For the other metals,

even though the open circuit potentials were in fair agreement with the ranges of the theoretical potentials, further experimentation will be required to determine the reaction mechanisms involved (hence, the actual theoretical potentials of the cells) before any meaningful comparison can be made.

Because of the lack of information concerning the behavior of thin oxide films at high temperatures, no a priori statement could be made about the energy output of the various cells. However, one observation seems to be justified. Pauling (15, p. 350) gives the following values, in Angstroms, for the ionic radii of the anodic metals tested:

Mn^{++} : 0.80

Fe^{++} : 0.75

Co^{++} : 0.72

Ni^{++} : 0.70

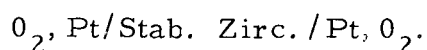
It will be noted that the radii of these ions are very nearly the same. Therefore, if it could be assumed that the activation energy required for the anodic reaction and transport of the metal ions through the oxide film was determined mainly by the temperature and the cationic radius, then, since the different ions are roughly the same size, the magnitude of the cell EMF would be the main factor in determining the relative values of the energy output for the different cells at the

same temperature. The observed energy values support these hypotheses since they increase with increasing open-circuit potential and theoretical EMF.

If an extrapolation is justified, one could predict that a much greater energy output would be realized from a cell with one of the more refractory metals as anode. For example, zirconium, yttrium, and thorium, all have much higher EMF's than the metals actually tested, and would therefore produce a greater amount of energy.

The Initial Prominence of the Discharge Curve

Figure 19 is a photograph of an oscilloscope trace³¹ taken while a pulsed current was being forced to flow through the cell



It shows that the cell polarization due to the internal resistive, activation, and concentration overpotentials is entirely realized in less than one millisecond after the current begins to flow or after it stops flowing. Other traces were obtained for the same cell but with the trace travelling across the scope at rates as slow as 0.2 seconds per centimeter. Behavior similar to that depicted in Figure 19 was observed in all cases. Successive traces with a total time up to 30 seconds produced only a slight increase in the magnitude of

³¹ Type 545A with CA dual trace preamplifier, Tektronix Incorporated, Portland, Oregon

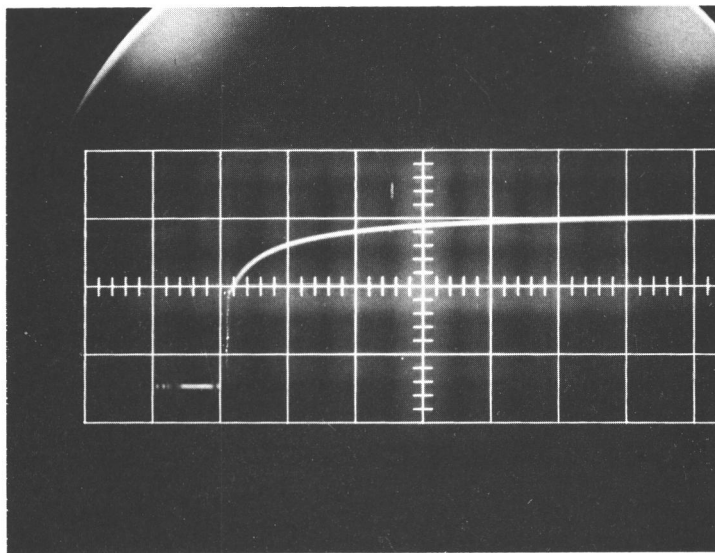


Fig. 19. Photograph of an oscilloscope trace obtained while forcing a current pulse through the cell $\text{O}_2, \text{Pt}/\text{Stab. Zirc.}/\text{Pt}, \text{O}_2$. The vertical scale is 0.05 volts/cm. The horizontal scale is 0.1 millisecond/cm. The small squares are one centimeter square.

the polarization at the end of the traces over that shown in Figure 19.

Hence, the initial prominence in the discharge curves for the iron, nickel, and cobalt cells is not a result of any of the three common overpotentials. Therefore, it must be concluded that something is occurring at the anode, other than the discharge of the anodic metal, to cause this phenomenon.

The anodic metal films appeared, under microscopic examination, to be impervious when compared with the platinum electrodes. During the recharging of any given cell, it was observed that more current was passed through the cell than could be accounted for by the recharging of the anodic metal alone. Since the electrolyte will only conduct oxygen ions, it must be concluded that the electrolyte itself is decomposed after the cell has been fully charged. Additional support for this conclusion is found in the following observations:

1. During the testing of the cobalt cell, the height and width of the initial prominence could be varied by varying the magnitude of the charging potential above that required for charging the cell. If the charging potential was held close to that theoretically required to decompose the cobalt oxide, then only a very small prominence was recorded. If, however, the charging potential was brought close to the theoretical EMF for the zirconium-oxygen couple, the prominence assumed essentially the same size as those obtained for the

iron and nickel cells where the charging potential was always of this approximate magnitude or higher.

2. If the anode film is non-porous, the only source of oxygen after the anodic oxide has been decomposed is the electrolyte itself.
3. If the cell was allowed to remain at open circuit after charging for an extended period of time, the length of which depended on the electronic conductivity and porosity of the cell, it would discharge internally down to the open-circuit potential characteristic of the cell. A cell was discharged after standing at open circuit for three minutes following the charging cycle. The potential-time and current-time curves were compared, respectively, with those obtained from a discharge through the same load immediately after charging. The flat section of the curves were identical. The initial prominence was very small for the delayed discharge. The fact that the curves were identical over their flat portions also lends support to the conclusion above, since if the main anode metal was being discharged instead of a decomposed portion of the electrolyte, the discharge curves could not be the same. Under any given operating conditions, the oxide film formed during discharge will have a fixed thickness for the same final current and cell potential. That is, for any

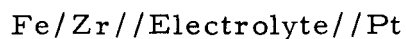
given operating conditions there is a fixed amount of power produced by a cell, hence a fixed amount of the anode is consumed. Any internal discharge would reduce this amount.

It can therefore be concluded that a species such as Zr , Zr_xCa_y , $Zr_xCa_yFe_z$, $Zr_{0.85}Ca_{0.15}^0$, etc., is formed at the anode during the recharging cycle, and subsequently discharges during the discharge cycle.

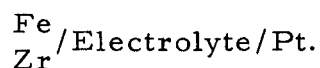
As has been stated previously, one must know when zero time occurs for a given cell's discharge in order to calculate the energy output of the cell.

To explore this problem further, suppose the cell being tested is an iron cell. If the cell has just been charged there is iron at the anode plus some other species having a higher EMF. With two anodic materials available for discharge in the same cell, one can postulate either a series, a parallel, or a series-parallel equivalent arrangement of batteries in a circuit. For the reaction to proceed, an electrolyte-electrode interface must be maintained. Therefore, all of the electrolyte that has been decomposed is adjacent to an electronic conductor--the metal anode being studied. Essentially no iron oxide would be present since its decomposition potential is lower than the decomposition potential of the electrolyte (the material having the lowest potential would be decomposed first, followed by other higher-

EMF species). If the other species were zirconium a series cell would appear as

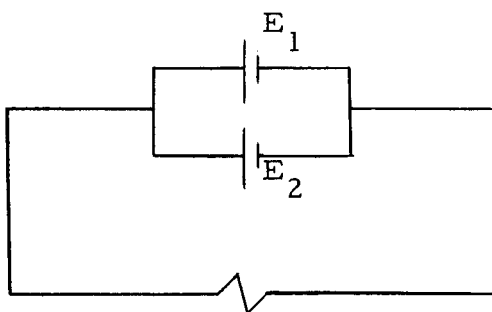


and a parallel cell would appear as



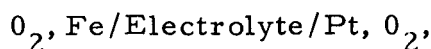
If the cell were completely of the series type, the iron would merely act as a collector and during discharge, the electrolyte-electrode interface would move through the zirconium to the iron. This series arrangement would very satisfactorily explain the experimental data (initial prominence) and would indicate that no iron would react until the zirconium had reacted.

If the cell were of the parallel type, its equivalent circuit would be



Let $E_1 > E_2$, e. g., $E_{Zr} > E_{Fe}$. As long as some decomposed electrolyte remains, the potential across both cells will be E_{Zr} . This has the effect of imposing a back-EMF on the iron cell which prevents it from discharging. The iron cell cannot begin to discharge until the two potentials are equal, that is, until all the zirconium has been consumed. Hence, we conclude for the parallel cell also, that no iron is consumed during the initial discharge of the cell as represented by the prominence in the discharge curve.

The phenomenon observed when the cell discharge cycle was delayed can also be explained with this parallel circuit. This indicates that the actual cell has some, possibly all, parallel character. The decay of the initial prominence in time with no current flowing through the external circuit indicates that an internal current exists, which is possible if either the iron oxide is not completely decomposed or the iron film is somewhat porous. The back-EMF applied to the iron cell by the decomposed electrolyte-oxygen couple is sufficient to drive a current through the iron cell in either case. It is unlikely that very much iron oxide is available when the cell has just been recharged. However, if the iron is porous, the iron cell would have the configuration



which could pass the current produced by the decomposed electrolyte-

oxygen cell, and hence, account for the above delay phenomenon.

These same arguments would apply to a combined series-parallel arrangement. It is therefore concluded that, for the purpose of the energy calculation, the cell discharge time begins after the decay of the initial prominence.

The fact that the manganese discharge curves do not exhibit this initial prominence does not invalidate the above arguments. The theoretical EMF of the manganese-oxygen couple is close to the open-circuit potential measured for the decomposed electrolyte in the other cells tested. Any overcharging would decompose the electrolyte in the manganese cell also. However, in this cell, the initial prominence would in a sense be a part of the cell discharge curves and would therefore represent useful available energy.³² This would have the effect of increasing the energy output over and above that realized from a pure manganese discharge.

³² A usual requirement for a battery is that its discharge curve should be as flat as possible and it is in this sense that the term useful available energy is used.

CONCLUSIONS

1. The feasibility of using stabilized zirconia as the electrolyte in a high temperature solid state battery was established. It was demonstrated that an air-depolarized solid battery having a useful life of three to five minutes could be fabricated. (An example of its application would be in the electrical power supply of a rocket during the initial firing period.)
2. Vacuum evaporation and deposition of an initial thin film of metal on the ceramic substrate followed by an electroplating (or electroless plating) operation to thicken the film was proven to be a successful method for preparing air-depolarized solid batteries.
3. Of the anodes tested, manganese produces the greatest amount of energy. The cobalt cell appears to have the longest life and the flattest discharge curves.
4. Because the measured open-circuit potentials are in good agreement with the theoretical values of the EMF for each cell (Table I), this solid state electrochemical device is useful for obtaining thermodynamic data for metallic oxides at high temperatures.
5. All cells tested could be recharged; hence, they could be classified as secondary batteries.

RECOMMENDATIONS FOR FUTURE STUDY

1. Impervious ten mole percent yttria-stabilized zirconia should be used for future work because of its lower resistivity.
2. Experiment with a heavier coating of the anode metal on a very thin section of the electrolyte, and coat the anode with platinum paste. This could possibly obviate the use of the back-EMF during the cell heat-up, and eliminate the initial prominence in the discharge curve.
3. A platinum-hydrogen anode should be used in order to study potential solid cathodic materials.
4. Build the air-depolarized, or completely solid batteries, using a plasma spray gun. (One might possibly find himself concerned with wettability here.) In this same manner, fabricate a battery of cells in a series arrangement. If this were successful, a battery could be built up having a high potential, a very low internal resistance and occupying a very small volume.
5. Instead of using spring-loaded contacts on the monitoring electrodes, it was found at the end of the project that if the monitoring electrodes were extended down the sides of the crucible (painted on with platinum paste) the electrodes could be easily connected to the external leads via small alligator clips. These were much easier to use than the spring-loaded contacts.

BIBLIOGRAPHY

1. Adams, David R. et al. Fuel cells, power for the future. Boston, Fuel Cell Research Associates, 1960. 160 p.
2. Archer, D.H. et al. An investigation of solid-electrolyte fuel cells, July 1963. Pittsburg, Pennsylvania, 1963. 66 numb. leaves. (Westinghouse Electric Company. Technical documentary report no. ASD-TDR-63-48)
3. Austin, B. O. et al. Thermally activated power cells. American Ceramic Society Bulletin 43:117-121. 1964.
4. Baur, Emil and Hans Preis. Über Brennstoff-Ketten mit Festleitern. Zeitschrift für Elektrochemie und angewandte Physikalische Chemie 44:727-732. 1937.
5. Blum, William and George B. Hogaboom. Principles of electroplating and electroforming (electrotyping). 3d ed. New York, McGraw-Hill, 1949. 455 p.
6. Burbank, R. B. and W. R. Hoskyns. Research on the thermal properties of zirconia, Sept. 1963. Alfred Station, New York, 1963. 72 numb. leaves. (Materiadyne, Aerospace Research Laboratories report no. ARL63-170)
7. Dietzel, A. and H. Tober. High-temperature reactions of zirconium oxide and twenty-nine binary systems with zirconium oxide. Deutsche keramische Gesellschaft 30:47-61. 1953.
8. Duwez, Pol, Francis Odell and Frank H. Brown, Jr. Stabilization of zirconia with calcia and magnesia. Journal of the American Ceramic Society 35:107-113. 1952.
9. Hund, F. Die Fluoritphase im System ZrO_2 -CaO. Zeitschrift für Physikalische Chemie 199:142-151. 1952.
10. Jasinski, R. J. and T. G. Kirkland. A state-of-the-art-report. Mechanical Engineering 86:51-57, 121-126. 1964.
11. Kingery, W. D. et al. Oxygen ion mobility in cubic $Zr_{0.85}Ca_{0.15}O_{1.85}$. Journal of the American Ceramic Society 42:393-398. 1959.

12. Kiukkola, Kalevi and Carl Wagner. Measurements on galvanic cells involving solid electrolytes. *Journal of the Electrochemical Society* 104:379-383. 1957.
13. Metal finishing guidebook directory. 32d ed. Westwood, New Jersey, Metals and Plastic Publications, 1964. 794 p.
14. Nernst, W. Über die elektrolytische Leitung fester Körper bei sehr hohen Temperaturen. *Zeitschrift für Elektrochemie* 6:41-43. 1899.
15. Pauling, Linus. The nature of the chemical bond. 2d ed. Ithaca, New York, Cornell University Press, 1940. 450 p.
16. Tien, T. Y. and E. C. Subbarao. X-ray and electrical conductivity study of the fluorite phase in the system $\text{ZrO}_2\text{-CaO}$. *The Journal of Chemical Physics* 39:1041-1047. 1963.
17. Tien, T. Y. The system $\text{ZrO}_2\text{-CaO}$: Electrical conductivity study in the two-phase regions, July 1, 1963. Pittsburgh, Pennsylvania, 1963. 7 numb. leaves. (Westinghouse Research Laboratories. Scientific paper no. 63-943-267-P3)
18. Trombe, Félix and Marc Foëx. Étude de la conductibilité électrique du système zircone-chaux à haute température. *Académie des sciences, Paris. Comptes rendus* 236:1783-1785. 1953.
19. Van Houten, G. R. A survey of ceramic-to-metal bonding. *American Ceramic Society Bulletin* 38:301-307. 1959.
20. Volchenikova, Z. S. and S. F. Pal'guev. Electric conductivity of solid oxide systems. II. System $\text{ZrO}_2\text{-CaO}$. Electric conductivity and transference numbers (Hittorf numbers). *Trudy Institute Elektrokhimii, Akademiya Nauk SSSR, Ural'skii Filial* 1:119-126. 1960.
21. Weissbart, J. and R. Ruka. A solid electrolyte fuel cell. *Journal of the Electrochemical Society* 109:723-726. 1962.
22. Wicks, Charles E. and Frank E. Block. Thermodynamic properties of 65 elements, their oxides, halides, carbides, and nitrides. 1963. 493 p. (U.S. Bureau of Mines. Bulletin 605)

APPENDIX I

Selection of Anodes

With an operating temperature of 1000° C and in a study concerned with electrodes in the solid state, there are many materials entirely unsuitable for experimentation. It was necessary, therefore, to examine some of the properties of the elements and their oxides to find those which would be suitable for use as anodes in this work.

Table II, constructed from published thermodynamic data (22), presents a few pertinent properties of some of the elements and their oxides. The asterisk to the right of the EMF values of some of the couples indicates the thermodynamically preferred oxide, hence EMF, as determined by the relative values of the free energy of the various reactions

$$\Delta F_f^O (\text{metal oxide})_i = \Delta F_f^O (\text{metal oxide})_j$$

One of the first things to be considered is the melting point of the pure metal. It of course must be greater than 1000° C. This immediately eliminates silver, aluminum, barium, calcium, cadmium, cesium, lanthanum, lithium, magnesium, lead, strontium, and zinc from further consideration (see Table II). Likewise, in considering the oxides of the remaining elements, boron and carbon are also eliminated because of low melting points. Even though beryllium is

satisfactory under the melting point criterion, it was not used because of the toxicity of its oxide. The melting point of copper is only slightly above 1000°C , so it was eliminated also.

The remaining list of metals is still quite large, and at first glance one might assume that it represented a very large number of satisfactory materials. However, the problems encountered in electroplating metals from their fused salt baths were considered to be sufficiently great to preclude the use of such techniques. Therefore, if one is limited to considering only those metals which can be electroplated from an aqueous bath, the list of acceptable materials is appreciably reduced, and includes only iron, nickel, chromium, manganese, and cobalt.

From the large list of metals requiring non-aqueous electroplating techniques, three metals were selected for experimentation. Molybdenum was selected as being somewhat representative of the remaining refractory metals. Also, evaporation of molybdenum in vacuum plating work is done from a pure molybdenum filament and it was felt that one might be able to deposit the entire anode film using this technique. Zirconium and yttrium were selected for an entirely different reason. Ten-mole percent yttria-stabilized zirconia is an oxygen-ion conductor and has a higher conductivity than the best calcia-stabilized zirconia at the same temperature (Figure 2). Therefore, if one could fabricate a cell using a solid solution of ten-mole

percent yttrium and 90-mole percent zirconium as the anode and if these metals reacted in that same ratio, the anodic reaction products formed during cell discharge would merely increase the thickness of the electrolyte and would, therefore, greatly reduce the anodic polarization during discharge. Hence, the list of anodic materials selected for this work consists of iron, nickel, chromium, cobalt, manganese, molybdenum, zirconium, and yttrium.

TABLE II. SOME THERMODYNAMIC PROPERTIES OF THE METALS AND THEIR OXIDES AT 1273°K

Material	mp, °C (22)	ΔF_f° , Kcal/mole (22)	EMF, volts*
Al	659		
Al ₂ O ₃	2040	303.8	2.196
Ag	961		
Ag ₂ O	positive free energy change		
Ag ₂ O ₂	positive free energy change		
Ba	710		
BaO	1923	104.2	2.26
Be	1283		
BeO	2550	113.5	2.46
B	2027		
B ₂ O ₃	450	230.7	1.67
Cd	321		
CdO	decomposes 900 to 1000	19.5	0.42
Ca	851		

*Calculated from Faraday's Law, ($EMF = \Delta F/n\mathcal{F}$)

TABLE II. (continued)

Material	mp, °C	ΔF_f° , Kcal/mole	EMF, volts
CaO	2600	120.6	2.62
C	3500		
CO	gaseous	53.8	1.17
CO ₂	gaseous	94.7	1.03
Cr	1900		
Cr ₂ O ₃	2280	192.7	1.39
Ce	804		
CeO ₂	2600	200.3	2.17*
Ce ₂ O ₃	1687	334.7	2.42
Co	1490		
CoO	1800	34.7	0.75*
Co ₃ O ₄		101.6	0.55
Cb (Nb)	2497		
CbO ₂		136.1	1.48
Cb ₂ O ₅	1512	323.7	1.40*
Cu	1084		
CuO	1447	10.8	0.23*
Cu ₂ O	1229	19.5	0.42

*Thermodynamically preferred oxide as determined from free energy considerations.

TABLE II. (continued)

Material	mp, °C	ΔF_f° , Kcal/mole	EMF, volts
Fe	1530		
$\text{Fe}_{0.95}\text{O}$	1377	42.8	0.928
Fe_2O_3	1457	118.5	0.857*
Fe_3O_4	1597	170.2	0.923
Hf	2215		
HfO_2	2790	208.1	2.26
La	920		
La_2O_3	2327		2.36@ 1200°K
Li	180		
Li_2O	1727	96.7	2.10
Mg	650		
MgO	2900	110.3	2.39
Mn	1244		
MnO	1785	69.6	1.51
Mn_2O_3	loses $1/2\text{O}_2$ @1080	145	1.05
Mn_3O_4	1590	224.2	1.22*
Mo	2610		
MoO_2	2227	84.9	0.92
MoO_3	795	106.4	0.77*
Nd	1024		

TABLE II. (continued)

Material	mp, °C	ΔF_f° , Kcal/mole	EMF, volts
Nd ₂ O ₃	no data		2.55@ 1200°K
Ni	1452		
NiO	1960	30.1	0.65
Pb	328		
PbO	886	22.98	0.5
Sc	1400		
Sc ₂ O ₃		314.9	2.28
Si	1410		
SiO ₂	1610	155.3	1.68
Sm	1052		
Sm ₂ O ₃		349.1	2.52
Sr	770		
SrO	2415	107.8	2.34
Ta	2996		
Ta ₂ O ₅	1877	356.8	1.55
Th	1695		
ThO ₂	2952	234.6	2.54
Ti	1725		
TiO	2020	95.1	2.06
Ti ₂ O ₃	2127	280.1	2.03

TABLE II. (continued)

Material	mp, °C	ΔF_f° , Kcal/mole	EMF, volts
TiO ₂	1850	170.7	1.85*
Ti ₃ O ₅	2227	453.3	1.97
W	3377		
WO ₂	1270	84.6	0.92
WO ₃	1470	125.4	0.91*
U	1132		
UO ₂	2727	207	2.25
U ₃ O ₈	1677	647.7	1.76*
V	1917		
VO	2077	71.6	1.55
V ₂ O ₃	1977	219.5	1.59
V ₂ O ₄	1545	240.98	1.31
V ₂ O ₅	670	249.8	1.08*
Y	1500		
Y ₂ O ₃	2227	362.5	2.62
Zn	420		
ZnO	1975	51.4	1.12
Zr	1852		
ZrO ₂	2677	204	2.21

APPENDIX II

Anode Film Construction

Iron Anode. Pure 36 gauge iron wire was wound around a loose-lay, three strand, tungsten wire, each strand being 0.030 inch in diameter. Because the temperature of the filament during the deposition process was greater than the melting point of iron, great care had to be exercised in using this filament. Otherwise, the iron would either run off of the tungsten filament, alloy with it and cause it to burn out, or splatter on the ceramic target. One filament was found to be sufficient for the iron plating process for each iron cell constructed.

A common chloride bath (13, p. 240) was used for the electroplating process. The electrolysis was carried out with a current density of about 80 ma/cm^2 , a bath pH of 0.8, and a bath temperature of 190° to 200° F. With 20 ohms resistance across the base of the cell, the electroplating process naturally occurred faster nearer the copper contacts. However, in a very short time there was sufficient iron plated on the vapor deposited base to allow the electroplating to occur uniformly across the entire base of the crucible.

After a sufficient amount of iron had been deposited, the cells were removed from the electroplating bath, dried, and a thin coat of oil applied to the iron anode to prevent chemical oxidation prior to the

actual testing of the cell.

Nickel Anode. For the vapor deposition of the nickel it was found necessary to deposit the nickel onto a tungsten basket. Without this intimate contact the filament temperature was excessively high. Consequently, nickel was electrodeposited on a tungsten basket in the common Watts-type (13, p. 264) nickel plating solution. During the electrodeposition process the pH was maintained at about 5 and the temperature at 115° to 160° F. When this filament was heated to its operating temperature in the vacuum chamber, it had a tendency to form hot spots which appeared to be caused by the alloying of the nickel with the tungsten. Unless careful temperature control was maintained, these hot spots burned through and ruined the filament. As many as three filaments were required to deposit a sufficient amount of nickel on the face of one crucible.

The above Watts solution was used also for the final electrodeposition of nickel on the vapor deposited base. It was found necessary to carry out the electroplating process at a rather low current density, approximately 20 ma/cm^2 . If a higher current density was used the deposit was pitted and burned. This rough deposit however, could be smoothed by additional electroplating at a lower current density.

Molybdenum Anode. Evaporation of molybdenum is generally accomplished by using a pure molybdenum filament. Since no aqueous

electroplating bath has been discovered for the electroplating of molybdenum, the complete anode would have to be formed using the vacuum deposition techniques. This was attempted and although it was easy to obtain an initial thin film, all attempts to bring the film to a thickness suitable for testing failed. Consequently no molybdenum cell was tested.

Zirconium and Yttrium Anodes. One is faced with the same problem here as with the molybdenum anodes in that no aqueous bath is available for electroplating these metals. Tungsten filaments were used and pieces of the metal to be deposited were placed inside the filaments. Subsequently, the usual vacuum plating techniques were employed. The molten metals wetted the tungsten filaments and the plating process was successful. One filament was all that was necessary to bring the resistance of the deposited film to approximately 15 ohms, and it appeared that a cell using these metals and/or mixtures of these metals could be constructed. However, at the end of this plating process, that is, when the resistance was approximately 10 to 15 ohms, all the zirconium and yttrium was completely evaporated from the filament. Consequently it was necessary to open the vacuum system and place a new supply of metal in the filament. When the vacuum chamber was opened the resistance across the film on the ceramic substrate immediately jumped to a very high value and

the major portion of the film became somewhat powdery. This phenomenon appeared to be caused by a partial oxidation of the metal. Both yttrium and zirconium are very reactive in the finely divided state. In fact, zirconium powder in a finely divided state is pyrophoric in air. This problem made it impossible to construct a cell using these metals as the anode. Major modifications in the equipment used would have to be made in order to fabricate this cell. It would be necessary to bring the anode to test thickness by continuously depositing the metal without opening the vacuum system during the process. Also it would probably be necessary to use two filaments (one containing zirconium and one containing yttrium) to construct such an anode.

Manganese Anode. Manganese was first deposited onto the zirconia crucible from a tungsten filament. The final resistance of the vacuum deposited film was approximately 25 ohms. The anode film was then brought to a thickness sufficient for testing by electroplating manganese from an aqueous bath (5, p. 353). The electroplating was carried out at approximately 26°C , and 150 to 200 ma/cm^2 current density. A good deposit was obtained and the cell was subsequently tested.

Cobalt Anode. Cobalt metal was evaporated from a tungsten filament. The final resistance of the deposited film was approximately

15 ohms. As usual it was necessary to bring this metal film to a thickness sufficient for testing. This was accomplished by immersing the base of the crucible in an electroless cobalt plating solution (13, p. 422). The pH was increased to 9 to 10 with ammonia and the solution was brought to a temperature of about 93° C. It was observed that the resistance of the deposited film then increased to about 200 ohms due to flaking off or some other dissolution of the anode film. However, the crucible was left in this solution for about one-and-one-half to two hours. At the end of this time it was observed that the resistance was down to about 3 ohms and a smooth plate had been achieved. A new solution was prepared and the crucible was immersed in this solution for about two-and-one-half hours. In both cases the bath was maintained at 93° C during the entire process. This process produced a satisfactory cobalt electrode and the cell was subsequently tested.

Chromium Anode. Chromium metal was evaporated from a tungsten filament. It was necessary to bond the chromium to the tungsten prior to the evaporation process. Otherwise the filament temperature had to be excessively high to heat the chromium to its evaporation temperature. The bonding was accomplished by melting the chromium onto the tungsten in a helium atmosphere, and the filament thus prepared was used to deposit the first thin film of

chromium on the zirconia crucible.

For the second stage of the anode build-up, electroplating chromium from a CrO_3 - SO_4 bath (13, p. 216) was attempted first. All attempts to build up the anode electrolytically were unsuccessful. In some cases, the resistance across the vapor-deposited film would increase to a value too high for plating to occur immediately upon immersion of the crucible into the bath. In all cases, whether the above phenomenon occurred immediately or over a longer period of time, it was not possible to effect the deposition of the chromium electrolytically.

Because of the success realized in plating cobalt from an electroless bath, even though part of the vapor-deposited film had been destroyed when the crucible was immersed into the bath, attempts were made to build up the chromium anode in an electroless chromium bath (13, p. 422). These attempts were also unsuccessful. Consequently, no chromium cell could be tested.